International Journal of Biological Macromolecules

Kinetic characterization of the oxIdation of catecolamines and related compounds by laccase

--Manuscript Draft--

Manuscript Number:	IJBIOMAC-D-20-01300R3
Article Type:	Research Paper
Section/Category:	Proteins and Nucleic acids
Keywords:	Laccase; kinetic; catecholamines
Corresponding Author:	Jose Jose Luis Northumbria University Newcastle Upon Tyne, Tyne and WEar UNITED KINGDOM
First Author:	Jesus Manzano-Nicolas
Order of Authors:	Jesus Manzano-Nicolas
	Amaury Taboada-Rodriguez
	Jose-Antonio Teruel-Puche
	Fulgencio Marin-Iniesta
	Francisco Garcia-Molina
	Francisco Garcia-Canovas
	Jose Tudela-Serrano
	Jose Jose Luis
Abstract:	The pathways of melanization and sclerotization of the cuticle in insects are carried out by the action of laccases on dopamine and related compounds. In this work, the laccase action of Trametes versicolor (TvL) on catecholamines and related compounds has been kinetically characterized. Among them, dopamine, L-dopa, L-epinephrine, L-norepinephrine, L-isoprenaline L-α-methyldopa and L-dopa methylester. A chronometric method has been used for this characterization, with the help of a small amount of ascorbic acid. The use of TvL has allowed docking studies of these molecules to be carried out at the active site of this enzyme. The hydrogen bridge interaction between the hydroxyl oxygen at C-4 with His-458, and with the acid group of Asp-206, would make it possible to transfer the electron to the copper centre of the enzyme. The presence of an isopropyl group bound to nitrogen (isoprenaline) makes it especially difficult to catalyse. The formation of the ester (L-dopa methyl ester) practically does not affect catalysis. The addition of a methyl group (α-methyl dopa) increases the rate but decreases the affinity for catalysis. L-epinephrine and L-norepinephrine have a similar affinity to isoprenaline, but faster catalysis, probably due to the greater nucleophilic power of their phenolic hydroxyl.
Suggested Reviewers:	Dr. Ayelet Fishman afishman@tx.technion.ac.il
	Annette Rompel annetterompel@univie.ac.at
	Manuela Garcia-Morenoi Manuela.Garcia@uclm.es
Opposed Reviewers:	
Response to Reviewers:	

Dr. Jose Muñoz Muñoz
Microbial Enzymology Lab (MEL)
Dept. Applied Sciences
Northumrbia University
Ellison Building, Room 326
Ellison Place, NE1 8SG
Newcastle Upon Tyne (UK)

Newcastle upon Tyne, 10th July 2020

Dear Prof Aichun Dong
Editor
International Journal of Biological Macromolecules

We would like to thank all Reviewer's comments and, at the same, we would like to provide a point-by-point answer to all of his/her comments and indications.

REVIEWER 2

The Reviewer 2 comments that:

Comment 1: "The Abstract in the first page of the submission is still different from the other in the text".

As the maximum number of words is 200 words in the website, we adjusted the abstract to this amount. However, the essence is the same in both abstracts but less detailed results in the short one.

Thank you, in advance, for your attention and courtesy.

Sincerely yours,

Dr. Jose Luis Muñoz Muñoz

Dr. Jose Muñoz Muñoz
Microbial Enzymology Lab (MEL)
Dept. Applied Sciences
Northumrbia University
Ellison Building, Room 326
Ellison Place, NE1 8SG
Newcastle Upon Tyne (UK)

Newcastle upon Tyne, 10th July 2020

Dear Prof Aichun Dong
Editor
International Journal of Biological Macromolecules

We would like to thank all Reviewer's comments and, at the same, we would like to provide a point-by-point answer to all of his/her comments and indications.

REVIEWER 2

The Reviewer 2 comments that:

Comment 1: "The Abstract in the first page of the submission is still different from the other in the text".

As the maximum number of words is 200 words in the website, we adjusted the abstract to this amount. However, the essence is the same in both abstracts but less detailed results in the short one.

Thank you, in advance, for your attention and courtesy.

Sincerely yours,

Dr. Jose Luis Muñoz Muñoz

1. ABSTRACT

The pathways of melanization and sclerotization of the cuticle in insects are carried out by the action of laccases on dopamine and related compounds. In this work, the laccase action of *Trametes versicolor* (TvL) on catecholamines and related compounds has been kinetically characterized. Among them, dopamine, L-dopa, L-epinephrine, L-norepinephrine, DL-isoprenaline, L-isoprenaline, DL-α-methyldopa, L-α-methyldopa and L-dopa methylester. A chronometric method has been used, which is based on measuring the lag period necessary to consume a small amount of ascorbic acid, added to the reaction medium.

The use of TvL has allowed docking studies of these molecules to be carried out at the active site of this enzyme. The hydrogen bridge interaction between the hydroxyl oxygen at C-4 with His-458, and with the acid group of Asp-206, would make it possible to transfer the electron to the T1 Cu-(II) copper centre of the enzyme. Furthermore, Phe-265 would facilitate the adaptation of the substrate to the enzyme through Π-Π interactions.

To kinetically characterize these compounds, we need to take into consideration that, excluding L-dopa, L-α-methyldopa and DL- α-methyldopa, all compounds are in hydrochloride form. Because of this, first we need to kinetically characterize the inhibition by chloride and, after that, calculate the kinetic parameters K_M and V^S_{max}.

From the kinetic data obtained, it appears that the best substrate is dopamine. The presence of an isopropyl group bound to nitrogen (isoprenaline) makes it especially difficult to catalyse. The formation of the ester (L-dopa methyl ester) practically does not affect catalysis. The addition of a methyl group (α-methyl dopa) increases the rate but decreases the affinity for catalysis. L-epinephrine and L-norepinephrine have an

affinity similar to isoprenaline, but faster catalysis, probably due to the greater nucleophilic power of their phenolic hydroxyl.

TITLE

Kinetic characterization of the oxidation of catecolamines and related compounds by laccase

AUTHORS

Jesus Manzano-Nicolas[a], Amaury Taboada-Rodriguez[a], Jose-Antonio Teruel-Puche[b], Fulgencio Marin-Iniesta[a], Francisco Garcia-Molina[c], Francisco Garcia-Canovas[c], Jose Tudela-Serrano[c] and Jose-Luis Muñoz-Muñoz[d*].

ADDRESSES

[a]Group of research Food Biotechnology-BTA (www.um.es/bta/), Department of Food Technology, Nutrition and Bromatology, Regional Campus of International Excellence "Campus Mare Nostrum", University of Murcia, E-30100, Espinardo, Murcia, Spain.

[b]Group of Molecular Interactions in Membranes (https://www.um.es/grupos/grupo-interacciones-moleculares/), Department of Biochemistry and Molecular Biology-A, Regional Campus of International Excellence "Campus Mare Nostrum", University of Murcia, E-30100, Espinardo, Murcia, Spain.

[c]GENZ-Group of research on Enzymology (www.um.es/genz), Department of Biochemistry and Molecular Biology-A, Regional Campus of International Excellence "Campus Mare Nostrum", University of Murcia, E-30100, Espinardo, Murcia, Spain.

[d]Department of Applied Sciences, Northumbria University, Newcastle Upon Tyne NE1 8ST, Tyne & Wear, England, United Kingdom.

*Corresponding Author: jose.munoz@northumbria.ac.uk (J-L. Muñoz-Muñoz). Microbial Enzymology Lab (MEL), Department of Applied Sciences, Northumbria University, Newcastle Upon Tyne NE1 8ST, Tyne & Wear, England, United Kingdom.

ORCID AUTHORS

Prof. Dr. Fulgencio Marin-Iniesta: https://orcid.org/0000-0002-9642-0266
https://publons.com/researcher/2485870/fulgencio-h-marin-iniesta/
Prof. Dr. Jose-Antonio Teruel-Puche: www.orcid.org/0000-0003-2256-3368
https://publons.com/researcher/1861660/jose-antonio-teruel-puche
Prof. Dr. Francisco Garcia-Canovas: www.orcid.org/0000-0002-8869-067X
https://publons.com/researcher/2481703/francisco-garcia-canovas

Prof. Dr. Jose Tudela-Serrano: www.orcid.org/0000-0002-5528-4296
https://publons.com/researcher/1414553/jose-tudela

Prof. Dr. Jose Luis Muñoz-Muñoz: www.orcid.org/0000-0003-0010-948X
https://publons.com/researcher/1413151/jose-munoz-munoz/

KEYWORDS

Laccase, kinetic, catecholamines, kinetic characterization, docking.

HIGHLIGHTS

- A chronometric method has been applied to characterize the action of laccase on catecholamines and related compounds.
- From lag-phase experimental recordings, steady-state rates have been determined.
- Non-linear regression of steady-state rates gave us the kinetic parameters V_{max} and K_M for each substrate.
- Laccase inhibition by chloride has been characterized.

1. ABSTRACT

The pathways of melanization and sclerotization of the cuticle in insects are carried out by the action of laccases on dopamine and related compounds. In this work, the laccase action of *Trametes versicolor* (TvL) on catecholamines and related compounds has been kinetically characterized. Among them, dopamine, L-dopa, L-epinephrine, L-norepinephrine, DL-isoprenaline, L-isoprenaline, DL-α-methyldopa, L-α-methyldopa and L-dopa methylester. A chronometric method has been used, which is based on measuring the lag period necessary to consume a small amount of ascorbic acid, added to the reaction medium.

The use of TvL has allowed docking studies of these molecules to be carried out at the active site of this enzyme. The hydrogen bridge interaction between the hydroxyl oxygen at C-4 with His-458, and with the acid group of Asp-206, would make it possible to transfer the electron to the T1 Cu-(II) copper centre of the enzyme. Furthermore, Phe-265 would facilitate the adaptation of the substrate to the enzyme through Π-Π interactions.

To kinetically characterize these compounds, we need to take into consideration that, excluding L-dopa, L-α-methyldopa and DL- α-methyldopa, all compounds are in hydrochloride form. Because of this, first we need to kinetically characterize the inhibition by chloride and, after that, calculate the kinetic parameters K_{Y} and V^{S}_{max}.

From the kinetic data obtained, it appears that the best substrate is dopamine. The presence of an isopropyl group bound to nitrogen (isoprenaline) makes it especially difficult to catalyse. The formation of the ester (L-dopa methyl ester) practically does not affect catalysis. The addition of a methyl group (α-methyl dopa) increases the rate but decreases the affinity for catalysis. L-epinephrine and L-norepinephrine have an

affinity similar to isoprenaline, but faster catalysis, probably due to the greater nucleophilic power of their phenolic hydroxyl.

1. Introduction

Laccases (EC 1.10.3.2, *p*-diphenol: oxygen oxidoreductase) are a family of multicopper oxidases, which oxidize a wide range of substrates with molecular oxygen, including inorganic and aromatic substrates. Laccases can be found in fungi, bacteria, insects and plants (Asano et al., 2019; Balabanidou et al., 2018). Laccase from *Trametes versicolor* contain four copper ions, one located at T1 site near the surface of the protein and three others copper ions buried at T2 and T3 sites (Rulíšek and Ryde, 2013; Sakurai and Kataoka, 2007). The catalytic cycle begins with the abstraction of one electron from the substrate bound near T1 site. A total of four electrons are sequentially transferred to the buried T3 site to reduce an oxygen molecule to water (Kjaergaard et al., 2012; Rulíšek and Ryde, 2013; Shleev et al., 2012). The products of the enzymatic reaction are free radicals, which evolve through non-enzymatic reactions towards polymers. (Dana et al., 2017; Janusz et al., 2020; Kushwaha et al., 2018). These enzymes act in the formation and degradation of lignins and in the formation of melanins (Kobayashi and Higashimura, 2003). It has been described that stable protein oligomers are formed in the sclerotization process of insect cuticles, with the help of catecholamine oxidation products (Suderman et al., 2006). Also, laccase located in salivary glands is used by *Nephotettix cincticeps* to polymerize toxic compounds in nontoxic polymers (Hattori et al., 2005).

In insects, there are the routes of melanization and sclerotization and both are used for cuticle staining (Sugumaran and Barek, 2016). There are differences between melanin biosynthesis and sclerotization reactions. Therefore, catecholamines evolve in the melanin pathway through cyclization and low reaction with external nucleophiles, excluding the case of pheomelanins. However, in the sclerotization, a linkage with

proteins occurs forming a supramolecular structure (Andersen, 2010). In insects, melanization and sclerotization are initiated by the action of laccase on dopamine, which, through one-electron oxidation, produces semiquinones as the first product. (Arakane et al., 2005). Regarding the nature of melanins, there is a big difference between eumelanin and pheomelanin from mammals and insects. Eumelanins derive essentially from dopa. However, in insects, eumelanin and pheomelanin come from dopamine (Barek et al., 2018). Dopamine oxidation by laccase originates *o*-semiquinone, which evolve to an *o*-dopaminaquinone. From this, eumelanin and pheomelanin are formed (Barek et al., 2018).

There are two types of laccase in insects, type I (Zhang et al., 2018) and type II (Liu et al., 2018). The existence of two laccase 2 isoenzymes (laccase 2A and laccase 2B) has been described in many insects, including *Manduca sexta* (Dittmer et al., 2009) and *Bombyx mori* (Yatsu and Asano, 2009). It has been proposed that oxidation of catecholamines by laccases is the key step in insect cuticle formation (Asano et al., 2019; Balabanidou et al., 2018).

Purification, crystallization and determination of the 3D-structure of laccase from *Trametes versicolor,* TvL (Piontek et al., 2002), makes it possible to carry out studies on the structure-activity relationships of this enzyme, on several substrates (Kushwaha et al., 2018). Since the optimal pH of TvL is 4 (Manzano-Nicolas et al., 2019), the products of the enzymatic reaction, *o*-quinones, evolve through two routes, being unknown the proportion corresponding to each route (García-Moreno et al., 1991). Thus, there would be no real molar absorptivity to use. Therefore, the use of the chronometric method in the presence of ascorbic acid can be useful (Manzano-Nicolas et al., 2019). In this work the oxidation by TvL of catecholamines (CA) and related compounds (CR) is studied kinetically, using the previous chronometric method. To

obtain the real kinetic parameters, the inhibition by chloride has to be studied first due to the hydrochloride form of all compounds, except L-dopa, L-α-methyldopa and DL-α-methyldopa. In addition, studies are carried out on the docking of the different substrates at the active site of TvL, establishing structure-activity relationships.

2. Material and Methods

2.1 Materials

We used laccase from *Trametes versicolor* (TvL, Fluka 53739, Madrid, Spain, 8U/mg). The unit (U) of laccase activity is defined as the amount of enzyme that acting on 4-*tert*-butylcatechol (TBC) at 1 mM concentration, generates a micromole of product 4-tert-butyl-*o*-benzoquinone (TBQ) per minute, at pH = 4.0 in 50 mM sodium acetate buffer at 25ºC (activity = 0.9 ΔA_{410nm} micromoles/min) (Manzano-Nicolas et al., 2019). The molar absorptivity of TBQ at 410 nm in these conditions was 1100 $M^{-1}cm^{-1}$. DL-isoprenaline, L-isoprenaline, L-dopa methyl ester, dopamine, L-norepinephrine and L-epinephrine are in hydrochloride form and the inhibition by chloride has to be taking into consideration, Fig. 1SM. L-dopa, L-α-methyldopa and DL-α-methyldopa are not in hydrochloride form so we can exclude this inhibition. All above compounds were purchased from Sigma (Madrid, Spain) (Fig. 1). Ascorbic acid (AH_2) and 4-*tert*-butylcatechol (TBC) were also purchased from Sigma (Madrid, Spain). Stock solutions of these substrates were prepared in 0.15 mM acetic acid to prevent autoxidation. Milli-Q- system ultrapure water was used.

2.2 Methods

2.2.1 Laccase activity: Chronometric method.

The enzymatic activity of laccase on CA and CR was followed spectrophotometrically in the visible zone, measuring the formation of the corresponding products after the consumption of a determined amount of ascorbic acid (micromolar) by reaction with the *o*-semiquinones generated by the enzyme. Since in all cases the product absorbs in the visible area, the classic chronometric method is used,

since the AH_2 spectrum does not influence the measurement (Manzano-Nicolas et al., 2019; Munoz et al., 2006; Rodriguez-Lopez et al., 2000). Except where otherwise indicated, the experimental conditions were: pH 4.0, 50 mM acetate buffer and 25ºC.

2.2.2. ^{13}C NMR assays.

^{13}C NMR spectra of catecholamines and related compounds study were obtained on a Varian unity spectrometer of 300 MHz, using $^{2}H_2O$ as solvent for the substrates. δ-values were measured relative to those for tetramethylsilane (δ=0). The maximum wide line accepted in the NMR spectrum was 0.06 Hz, so that the maximum accepted error for each peak was ± 0.03 ppm (Manzano-Nicolas et al., 2019). The dependence of δ values in ^{13}C for a carbon atom on its electron density is known (Farnun, 1975; Günther, 1980). Moreover, the electron-donating capacity of the oxygen atom from different phenolic compounds (nucleophilic power) has been correlated with the experimental δ values in ^{13}C for the carbon atom that supports the hydroxyl group (Shogo et al., 1993).

2.3 Computational docking.

Molecular docking was carried out around T1 copper of laccase with all substrates used in the kinetic study. The chemical structures information for all substrates are available in the PubChem Substance and Compound database (https://pubchem.ncbi.nlm.nih.gov) (Kim et al., 2016) through the unique chemical structure identifier CID 681 for dopamine, 6047 for L-dopa, 5816 for L-epinephrine, 439260 for L-norepinephrine, 5808 for D-isoprenaline, 443372 for L-isoprenaline, 721860 for D-α-methyldopa, 38853 for L-α-methyldopa and 23497 for L-dopa methylester. In all cases molecules were modified to be in the ionic form, and Gasteiger atom charges were assigned. The molecular structure of laccase was taken from the Protein Databank (PDB ID: 1GYC) (Piontek et al., 2002), corresponding to laccase

from the *Fungus Trametes versicolor* at 1.90 Å resolution. Input protein structure for docking was prepared by adding all hydrogen atoms and removing non-functional water molecules. Rotatable bonds in the substrates and Gasteiger's partial charges were assigned by AutoDockTools4 software (Morris et al., 2009; Sanner, 1999).

AutoDock 4.2.6 (Morris et al., 2009) package was employed for docking. Lamarkian Genetic Algorithm was chosen to search for the best conformers. The maximum number of energy evaluations was set to 2,500,000, the number of independent docking to 200 and the population size to 150. Grid parameter files were built using AutoGrid 4.2.6 (Huey et al., 2007). The grid box was centred at T1 copper with a grid size set to 60x60x60 grid points with spacing of 0.375 Å. Other AutoDock parameters were used with default values. PyMOL 2.2.0 (www.pymol.org) and AutoDockTools4 (Morris et al., 2009; Sanner, 1999) were employed to edit and inspect the docked conformations. LigPLot software was used for two-dimensional representations (Wallace et al., 1995).

2.4 Statistical analysis of experimental data.

Steady state rates (V_{SS}) values are determined from the spectrophotometric recordings and these values are adjusted to the Michaelis-Menten equation providing the values of V_{max} and K_M. Data were recorded as mean ± standard deviation of at least triplicate determinations.

3. Results and Discussion

In this study, the action of laccase on CA and CR is studied (Fig. 1). The products of the reaction are *o*-semiquinones that evolve towards coloured compounds that absorb in the visible between 450-470 nm.

3.1 Characteristics of enzymatic reaction products.

In the action of laccase on CA and CR, free radicals (*o*-semiquinones) originate, which disproportionate as indicated in Fig. 2, originating *o*-quinones and regenerating the substrate. Two routes emerge from the protonated *o*-quinone (García-Moreno et al., 1991), the main one carries out the cyclization and the coupled oxidation/reduction, originating an aminochrome. The other route begins with the addition of water to the protonated *o*-quinone, generating a trihydroxy-compound, which in turn is oxidized by another *o*-quinone molecule, generating a *p*-topaquinone and regenerating the substrate. *p*-Topaquinone cycles very slowly towards aminochrome (Fig. 2). Thus, in the action of laccase on these compounds, an absorbance is produced due to a mixture of products: aminochrome and *p*-topaquinone, with a coefficient of molar absorptivity, of the mixture, unknown. Therefore, it is convenient to use the chronometric method, since what is measured, in this case, is time.

3.1.1 Deduction of analytical expression for the steady-state rate.

Lacasse action on CA and CR generates semiquinones, which evolve to aminochromes with the pass of the time, accumulating different intermediates, Fig. 2, and originating a lag-phase, which needs to be taking into consideration when the analytical expression for the steady-state rate is obtained. The rate of action of the enzyme in steady-state for a substrate S is V_{SS}^{S}, the matter that enters the medium is

V_{SS}^{S} t, accumulates in intermediates (*o*-semiquinones) that are reduced by AH_2, until it is depleted in the medium and this leads to the accumulation of *o*-quinones and the formation of the products dopachrome [DC] and *p*-topaquinone [PQ] (García-Moreno et al., 1991) (Fig. 2), according:

$$V_{SS}^{S}\,t = \sum[I] - 2\,[AH_2]_0 = 4\,([DC] + [PQ]) \qquad [1]$$

Where I are chemical intermediates that accumulate in the medium, $[AH_2]$ is the added ascorbic acid and [DC]/[PQ] are the concentrations of the final products that accumulate in the medium. The sum of the concentrations of intermediates is:

$$\sum I = [QH] + [Q] + [T] \qquad [2]$$

Where QH and Q are the protonated *o*-quinone, the deprotonated *o*-quinone and T is the trihydroxy-derivative of the protonated *o*-quinone.

The added AH_2 concentration is consumed by the reaction with the *o*-semiquinone causing a lag period, which is in addition to that caused by the chemical reactions that arise from the protonated *o*-quinone (QH).

Applying the steady-state approximation to intermediates QH, Q and T, their analytical expressions are obtained according to:

$$[\dot{Q}H] = V_{SS}^{S} + k_{-1}[H^+][Q] - k_1\,[QH] - k_c\,[Q] - k_2'[QH] - k_4[QH][T] = 0$$

$$[\dot{Q}] = k_1\,[QH] - (k_{-1}[H^+] + k_c)[Q] = 0 \qquad [3]$$

$$[\dot{T}] = k_2'[QH] - k_4[QH][T] = 0$$

Where $k_2' = k_2\ [H_2O]$. The term $k_3\ [QH]\ [L]$ has been replaced by $k_c\ [Q]$ in Eq. [3], since in the steady-state both terms are equivalent. From Eq. [3] the expressions of $[QH]$, $[Q]$ and $[T]$ in the steady-state are:

$$[QH]_{SS} = \frac{(k_{-1}\ [H^+]+k_c)V_{SS}^S}{2\ k_1 k_c + 2\ k_2'(k_{-1}\ [H^+]+\ k_c)}$$

$$[Q]_{SS} = \frac{k_1\ V_{SS}^S}{2\ \ k_1 k_c + 2\ k_2'(k_{-1}\ [H^+]+\ k_c)} \qquad [4]$$

$$[T]_{SS} = \frac{k_2'}{k_4}$$

Substituting in Eq. [1] we have:

$$V_{SS}^S\ t - \left[\frac{(k_1 + k_{-1}\ [H^+]+\ k_c)V_{SS}^S}{2\ k_1\ k_2 + 2k_2'\ (k_{-1}\ [H^+]+\ k_c)} + \frac{k_2'}{k_4}\right] - 2\ [AH_2] = \ 4\ ([DC] + [PQ]) \qquad [5]$$

From Eq. [5], it follows that DC and PQ accumulate according to an equation line:

$$([DL] + \ [PQ]) = \frac{V_{SS}^S}{4}\left[t - \left(\frac{k_1 + k_{-1}\ [H^+]+k_c}{2\ k_1\ k_c + 2\ k_2'\ (k_{-1}\ [H^+]+k_c)} + \frac{k_2'}{k_4\ V_{SS}^S} + \frac{2\ [AH_2]}{V_{SS}^S}\right)\right] \qquad [6]$$

Thus, the accumulation of products over time corresponds to a line whose slope is $V_{SS}^S/4$ and cut the time axis to a value t = τ. When $([DC] + \ [PQ]) = 0$, the lag phase is obtained τ, made explicit by Eq. [7]:

$$\tau = \frac{k_1 + k_{-1}[H^+]+k_c}{2k_1 k_c + 2k_2'(k_{-1}\ [H^+]+k_c)} + \frac{k_2'}{k_4 V_{SS}^S} + \frac{2[AH_2]}{V_{SS}^S} \qquad [7]$$

Since $k_c \gg k_1$ (Garcia-Carmona et al., 1982; Jimenez et al., 1985; Jimenez et al., 1986; Jimenez et al., 1984b; Serna Rodriguez et al., 1990), the previous equation becomes:

$$\tau = \frac{k_{-1}[H^+]+k_C}{2k_1k_C+2k_2'(k_{-1}[H^+]+k_C)} + \frac{k_2'}{k_4V_{SS}^S} + \frac{2[AH_2]}{V_{SS}^S} \quad [8]$$

In high pH values, Eq. [8] is transformed at Eq. [9]:

$$\tau = \frac{k_{-1}[H^+]+k_C}{2k_1k_C} + \frac{2[AH_2]}{V_{SS}^S} \quad [9]$$

Thus, the delay period at high pH has two components, one due to Q cyclization and the other due to the consumption of AH_2.

When the two routes of cyclization and addition of water pass at lower pH, as is the case of laccase, the delay period (τ) has two components, one due to the cyclization of quinone (Q) and the cyclization of *p*-topaquinone τ_C (lag cyclation, lag_C) Eq. [10], and another due to the consumption of AH_2, τ_{AH_2} Eq. [11].

$$lag_C = \tau_C = \frac{k_{-1}[H^+]+k_C}{2k_1k_C+2k_2'(k_{-1}[H^+]+k_C)} + \frac{k_2'}{k_4V_{SS}^S} \quad [10]$$

$$lag_{AH_2} = \tau_{AH_2} = \frac{2[AH_2]}{V_{SS}^S} \quad [11]$$

Therefore,

$$\tau_{total} = \tau_C + \tau_{AH_2} \quad [12]$$

Thus, the difference of $\tau_{total} - \tau_C$ corresponds to the lag in the ascorbic acid consumption (τ_{AH_2}) and therefore, from these values, the enzyme action rate can be obtained V_{SS}^S. According:

$$\tau_{total} - \tau_C = \frac{2[AH_2]}{V_{SS}^S} \quad [13]$$

Or:

$$V_{SS}^{S} = \frac{2[AH_2]}{\tau_{total} - \tau_C} \quad [14]$$

3.1.1.1 Choosing the measurement wavelength.

Laccase activity was tested on different CA and CR, spectrophotometric records show a maximum in the visible region in the 400-475 nm zone, Fig. 3. For all the molecules, 475 nm was chosen as the measurement wavelength. As indicated above, a small amount of AH_2 (µM) is added, the absorbance at 475 nm is recorded over time and from the lag period and according to the Eqs. [13] and [14] the value of V_{SS} can be obtained.

3.1.1.2 Choosing pH and temperature.

The experiments of the action of laccase on CA and CR were carried out in 50 mM acetate buffer at pH = 4.0, optimal for *Trametes versicolor* laccase and a temperature of 25ºC.

3.1.1.3 Substrate type considerations

Among the substrates studied, several groups can be established (Fig. 1): a) those that carry a free amino group in the side chain and do not carry a carboxyl group such as: dopamine and L-norepinephrine (Fig. 4A). b) Those with a free or esterified acid group: L-dopa, L-dopa methyl ester, L-α-methyldopa, DL-α-methyldopa (Fig. 4B). c) Those bearing the substituted amino group such as: L-isoprenaline, DL-isoprenaline and L-epinephrine (Fig. 4C).

The power of the nucleophilic attack by the nitrogen of the amino group determines the cyclization rate of the *o*-quinones of each substrate. The substrates of

group A (Fig. 4A) dopamine and L-norepinephrine, have the free amino group and do not have notable electronic influences, at the pH of the measurement they cycle slowly (García-Moreno et al., 1991; Jimenez et al., 1984a), this carries with it its wide participation in the lag period and the steady-state rate must be calculated according to Eq. [14].

In group B substrates L-dopa, DL-α-methyldopa and L-α-methyldopa (Fig. 4B), the nucleophilic attack at this pH = 4.0 is more potent by nitrogen than those in group A (Garcia-Carmona et al., 1982; Jimenez et al., 1986; Serna Rodriguez et al., 1990), but a lag is also generated (except L-dopa methyl ester) and its value must be taken into account, to correct according to Eq. [14] and get the rate value (V_{SS}^{S}).

In group C substrates (Fig. 4C), the power of nitrogen nucleophilic attack is great, they cycle rapidly and thus do not provide $\mathrm{lag_C}$ to the measure, the lag corresponds to the consumption of AH_2 (τ_{AH_2}) and thus the value of V_{SS}^{S} can be obtained according to Eq. [14], with $\mathrm{lag_C} \cong 0$ (Jimenez et al., 1985), in this group the L-dopa methyl ester must be included.

3.2 Kinetic parameters determination

3.2.1 Substrates type A and B.

The *o*-quinones of the substrates shown in Fig. 1 have different cyclization constants, as corresponds to their structure and chemical properties.

In the case of substrates type A, Fig. 1, as shown in the spectrophotometric assays of the activity of laccase on dopamine (Fig. 5) and norepinephrine (Fig. 2SM), because

the cyclization of *o*-quinone is slow, $\mathrm{lag_C}$ makes a significant contribution to total lag and therefore Eq. [14] must be taken into account for the calculation of V_{SS}^{S}.

In the case of type B substrates, L-dopa, L-α-methyldopa and DL- α-methyldopa, although their cyclization constants are greater than that of type A substrates, show considerable $\mathrm{lag_C}$ and therefore, the calculation of the rate according to the chronometric method must be done by applying Eq. [14]. The experimental records are shown in Fig. 3SM (L-α-methyldopa), Fig. 4SM (DL- α-methyldopa) and Fig. 5SM (L-dopa).

For the L-dopa methyl ester substrate, methyl exerts an inductive effect and makes the amino group nitrogen more nucleophilic and therefore with a higher cyclization constant. This makes the contribution of the cyclization process in this case negligible and thus $\mathrm{lag_C} \cong 0$ ($\square_C \cong 0$), the rate calculation must be done according to Eq. [14], Fig. 6SM (L-dopa methyl ester).

3.2.2 Substrates type C.

To this group belong the type C substrates of Fig. 1, L-isoprenaline, DL-isoprenaline (Fig. 7SM) and L-epinephrine. The calculation of the steady state velocity must be obtained according to Eq. [14], with $\mathrm{lag_C} \cong 0$ ($\square_C \cong 0$).

3.2.3. Calculation of $\mathbf{V_{max}^{S}}$ and $\mathbf{K_M^{S}}$.

In all cases (substrates type A, B and C), the steady-state rate values are fit by non-linear regression to the Michaelis equation, and the values of K_M^S and V_{max}^S can be

obtained. In the case of substrates in hydrochloride form, these values are apparent by the chloride inhibition (see Supplementary Material, Fig. 6 and Fig. 7).

3.2.3.1 Substrates that are not in the form of salt.

This is the case of: L-dopa (Fig. 6), L-α-Methyldopa and DL- α-Methyldopa (Fig. 7). The kinetic parameters, obtained by non-linear regression to Michaelis equation, are directly K_M^S and V_{max}^S and are shown in Table 1. These values for the stereoisomers L-α-Methyldopa and DL- α-Methyldopa are almost identical, indicating that the enzyme is not stereoselective in its bond with the substrate or in catalysis. The smaller size of the side chain in the case of L-dopa, could be responsible for the increase in affinity (lower K_M^S, Table 1), at the same time, the lower hydrophobicity (absence of the methyl group) could be responsible for the lower value of V_{max}^S for worse adaptation in the active site. Note that the values of δ_1 are practically the same (Table 1).

3.2.3.2 Substrates that are in the form of salt.

Most of the substrates studied in this work are in the form of hydrochloride: L-isoprenaline, DL-isoprenaline (Fig. 6), L-dopa methyl ester, dopamine, L-norepinephrine and L-epinephrine (Fig. 7).

Chloride is known to be a laccase inhibitor (Raseda et al., 2014), recently a binding to the copper centre T2 has been proposed (Polyakov et al., 2019) and, in consequence, the inhibition should be mixed-type (see Supplementary Material) (Raseda et al., 2014). Furthermore, when the substrate concentration is varied to calculate the kinetic parameters of the enzyme, the inhibitor is being varied stoichiometrically and therefore the analysis of V_{SS}^S *vs.* $[S]_0$, according to Michaelis

equation (Eq. [7SM]), provides apparent data ($K_M^{S,app}$ and $V_{max}^{S,app}$) (Fig.6 and Fig.7, see Supplementary Material).

In this case, to calculate the real parameters K_M^S and V_{max}^S, we propose the following experimental design:

The inhibitor must first be characterized: type of inhibitor and strength of inhibition. To carry out the above, a substrate is chosen that is easily measurable, such as 4-tert-butylcatechol (TBC).

Step 1. Determine under experimental conditions equal to that of the inhibition tests the kinetic parameters of the substrate (TBC) (Fig. 8A), K_M^{TBC} and V_{max}^{TBC} resulting K_M^{TBC} = 0.28 ± 0.01 mM and V_{max}^{TBC} = 3.25 ± 0.02 μM/s.

Step 2. At different inhibitor concentrations repeat Step 1; determine $K_M^{TBC\,app}$ and $V_{max}^{TBC\,app}$ (Fig. 8A).

Step 3. Analyse $V_{max}^{TBC\,app}$ respect to the inhibitor concentration and determine K_I' (Eq. [2SM]) (Fig. 8B), the dissociation constant of the complex ESI (see Supplementary Material), resulting K_I' = 48.78 ± 8.49 mM.

Step 4. Analyse $K_M^{TBC\,app} - K_M^{TBC}$ values (Eq. [4SM]) respect to the inhibitor concentration (Fig. 8B). Therefore, the calculation of K_I, the dissociation of constant of the EI complex, with a value of K_I = 1.76 ± 0.05 mM.

Known K_I and K_I', a large difference in values can be observed, $K_I' > K_I$ and, in consequence, as we work under low values of substrate concentration, chloride

concentration values will be low and therefore competitive behaviour can be practically observed.

Step 5. From Eq. [7SM], $K_M^{S,app}$ and $V_{max}^{S,app}$ can be obtained. $K_M^{S,app}$ expression (Eq. [8SM]), knowing K_I, allows the calculus of K_M^S and, knowing the values of e $V_{max}^{S,app}$, K_M^S, and K_I, V_{max}^S can be obtained (Eq.[9SM]). Table 1 shows the values obtained.

From the data shown in Table 1, it can be deduced that the presence of a negative charge in the substrate (L-α-methyldopa, DL- α-methyldopa and L-dopa) causes an increase in the K_M^S, when L-dopa is esterified, the Michaelis constant decreases (L-dopa methyl ester). The compounds that carry the substituted amino group are: L-isprenaline, DL-isoprenaline and L-epinephrine show a low V_{max}, while the compounds with the free amino group show higher values of V_{max}. It is noteworthy that dopamine (physiological substrate) behaves kinetically as the best substrate for laccase.

3.3 Molecular docking.

It has been reported that T1 copper site directly interacts with the substrates through a hydrogen bond with a histidine (Christensen and Kepp, 2014), which is His-458 in laccase from *Trametes versicolor* 1GYC (Piontek et al., 2002). Specific mutations, within the substrate-binding site of this laccase, suggests that Asp-206 interacts directly with substrates (Christensen and Kepp, 2014; Madzak et al., 2006).

In this work it has been demonstrated the role of all ligands as substrates and, consequently as possible competitive inhibitors of physiological substrates. Accordingly, among the entire protein structure, only the structural region of substrate binding that can lead to catalysis has been explored, that is the T1 copper site region.

Docking conformations are selected according to the minimum free energy criteria after a cluster analysis in the T1 copper region. Fig. 9 shows the docking conformations of all substrates studied. All substrates adopt similar conformations in the more rigid part of the molecule structure, namely the phenyl ring containing the hydroxyl groups. The amino tail appears to be more flexible and can be found in different positions. This substituent is the cause of the most significant differences between substrates since different interactions with the protein can occur. Binding energies and the corresponding equilibrium dissociation constant are shown in Table 1. A quite good correlation is obtained between Michaelis constants values calculated from the kinetic analysis and the equilibrium dissociation constant from docking.

In order to explore in more detail the interactions of substrates with laccase the case of dopamine is chosen as a representative example (Fig. 10). The position of the phenyl ring is located at 4.8 Å almost parallel to the phenyl ring of Phe-265 allowing π-π stacking interactions stabilizing the substrate conformation. Thus, phenolic groups approach to His-458 and Asp-206. The carboxyl group of Asp-206 is located at 1.7 Å from the hydroxyl group in C-3 of dopamine and at 2.2 Å from the hydroxyl group in C-4. The hydroxyl group of C-4 is also close to a nitrogen atom of His-458. In all cases, these atoms are at distances where hydrogen bonds interactions can be established. It is worth noting that the proximity of the phenolic group to His-458 might allow electron transfer to T1 copper through His-458 in the oxidation reaction of the substrate in the catalysis (Christensen and Kepp, 2014). Besides, the amino tail helps to anchor dopamine in the active site by hydrogen bonds with Pro-163 and Phe-162. Fig.11 shows a 2D representation of Fig. 10. Discrepancies in the distance values are because in Fig. 11 polar hydrogen atoms are omitted, and the shown distances are calculated from oxygen atoms of dopamine instead of hydrogen atoms.

Fig. 12 shows a surface representation of Fig. 10. It can be seen that there is a large enough cavity in the surface of the protein to allocate the substrate near the T1 copper region and, thus, initiate the electron transfer from T1 copper to T3 coppers and finally to oxygen molecule.

4. Conclusions

The application of a chronometric method that uses AH_2 in micromolar quantities, allows obtaining the steady state speeds (V_{ss}^{s}), in the action of laccase acting on catecholamines and related compounds. Kinetic characterization of the inhibition by chloride allows to obtain the values of K_I and K_I' (Fig. 1SM) and, with the values of V_{ss}^{s}, the kinetic parameters K_M^S and V_{max}^S can be determined. Among all the substrates studied, the highest catalytic power (V_{max}^S/K_M^S) was for dopamine, physiologically related to melanization and sclerotization in the insect cuticle. The results of the docking of the substrates to the enzyme are in good agreement with the values of K_M^S. All the studied molecules could be oxidized by the same mechanism, with the participation of His-458, Asp-206 and Phe-265, facilitating the adaptation of the substrate to the active site, and allowing the transfer of electrons to T1 copper to via His-458.

Conflict of interest

The authors declare no conflict of interest and funds.

Acknowledgments

This work was partially supported by several grants, FEDER RTC-2017-5964-2 InsectFlour project "Aprovechamiento de subproductos industriales agrícolas para la producción de harinas de insectos para consumo humano y animal"/"Exploitation of industrial agronomic by-products to the production of insect flours for human and animal consumption" from Ministerio de Ciencia, Innovacion y Universidades (Madrid, Spain), 20961/PI/18 project and 20809/PI/18 project from Fundacion Seneca (CARM, Murcia, Spain), SAF2016-77241-R from MINECO (Madrid, Spain) and AEIP-15452 project from University of Murcia (Murcia, Spain). JMN has a research contract from RTC-2017-5964-2 project. JM-M receives internal funding from Northumbria University.

References

Andersen, S.O. (2010). Insect cuticular sclerotization: A review. Insect Biochemistry and Molecular Biology *40*, 166-178.

Arakane, Y., Muthukrishnan, S., Beeman, R.W., Kanost, M.R., and Kramer, K.J. (2005). *Laccase 2* is the phenoloxidase gene required for beetle cuticle tanning. Proceedings of the National Academy of Sciences of the United States of America *102*, 11337-11342.

Asano, T., Seto, Y., Hashimoto, K., and Kurushima, H. (2019). Mini-review an insect-specific system for terrestrialization: Laccase-mediated cuticle formation. Insect Biochemistry and Molecular Biology *108*, 61-70.

Balabanidou, V., Grigoraki, L., and Vontas, J. (2018). Insect cuticle: a critical determinant of insecticide resistance. Current Opinion in Insect Science *27*, 68-74.

Barek, H., Sugumaran, M., Ito, S., and Wakamatsu, K. (2018). Insect cuticular melanins are distinctly different from those of mammalian epidermal melanins. Pigment Cell & Melanoma Research *31*, 384-392.

Christensen, N.J., and Kepp, K.P. (2014). Setting the stage for electron transfer: Molecular basis of ABTS-binding to four laccases from Trametes versicolor at variable pH and protein oxidation state. Journal of Molecular Catalysis B: Enzymatic *100*, 68-77.

Dana, M., Bakhshi Khaniki, G., Mokhtarieh, A.A., and Davarpanah, S.J. (2017). Biotechnological and industrial applications of laccase: A Review. Journal of Applied Biotechnology Reports *4*, 675-679.

Dittmer, N.T., Gorman, M.J., and Kanost, M.R. (2009). Characterization of endogenous and recombinant forms of laccase-2, a multicopper oxidase from the tobacco hornworm, *Manduca sexta*. Insect Biochemistry and Molecular Biology *39*, 596-606.

Farnun, D.G. (1975). Charge density-NMR chemical shift correlationsin organic ions. Advances in Physical Organic Chemistry *11*, 123-173.

Garcia-Carmona, F., Garcia-Canovas, F., Iborra, J.L., and Lozano, J.A. (1982). Kinetic-study of the pathway of melanization between L-dopa and dopachrome. Biochimica Et Biophysica Acta *717*, 124-131.

García-Moreno, M., Rodríguez-López, J., Martínez-Ortiz, F., Tudela, J., Varón, R., and García-Cánovas, F. (1991). Effect of pH on the oxidation pathway of dopamine catalyzed by tyrosinase. Archives of Biochemistry and Biophysics *288*, 427-434.

Günther, H. (1980). Nuclear magnetic resonance of fluorine-19 and carbon-13 Ir. In NMR Spectroscopy (New York: John Wiley & Sons), pp. 364-374.

Hattori, M., Konishi, H., Tamura, Y., Konno, K., and Sogawa, K. (2005). Laccase-type phenoloxidase in salivary glands and watery saliva of the green rice leafhopper, *Nephotettix cincticeps*. Journal of Insect Physiology *51*, 1359-1365.

Huey, R., Morris, G.M., Olson, A.J., and Goodsell, D.S. (2007). A semiempirical free energy force field with charge-based desolvation. Journal of Computational Chemistry *28*, 1145-1152.

Janusz, G., Pawlik, A., Świderska-Burek, U., Polak, J., Sulej, J., Jarosz-Wilkołazka, A., and Paszczyński, A. (2020). Laccase properties, physiological functions, and evolution. International Journal of Molecular Sciences *21*, 966.

Jimenez, M., Garcia-Canovas, F., Garcia-Carmona, F., Iborra, J.L., and Lozano, J.A. (1985). Isoproterenol oxidation by tyrosinase - intermediates characterization and kinetic-study. Biochemistry International *11*, 51-59.

Jimenez, M., Garcia-Canovas, F., Garcia-Carmona, F., Lozano, J.A., and Iborra, J.L. (1984a). Kinetic-study and intermediates identification of noradrenaline oxidation by tyrosinase. Biochemical Pharmacology *33*, 3689-3697.

Jimenez, M., Garcia-Canovas, F., Garcia-Carmona, F., Tudela, J., and Iborra, J.L. (1986). Study of α-methyldopa oxidation by tyrosinase. Int J Biochem *18*, 39-47.

Jimenez, M., Garcia-Carmona, F., Garcia-Canovas, F., Iborra, J.L., Lozano, J.A., and Martinez, F. (1984b). Chemical intermediates in dopamine oxidation by tyrosinase, and kinetic studies of the process. Archives of Biochemistry and Biophysics *235*, 438-448.

Kim, S., Thiessen, P.A., Bolton, E.E., Chen, J., Fu, G., Gindulyte, A., Han, L., He, J., He, S., Shoemaker, B.A*., et al.* (2016). PubChem substance and compound databases. Nucleic Acids Research *44*, D1202-D1213.

Kjaergaard, C.H., Durand, F., Tasca, F., Qayyum, M.F., Kauffmann, B., Gounel, S., Suraniti, E., Hodgson, K.O., Hedman, B., Mano, N*., et al.* (2012). Spectroscopic and crystallographic characterization of "alternative resting" and "resting oxidized" enzyme forms of bilirubin oxidase: Implications for activity and electrochemical behavior of multicopper oxidases. Journal of the American Chemical Society *134*, 5548-5551.

Kobayashi, S., and Higashimura, H. (2003). Oxidative polymerization of phenols revisited. Progress in Polymer Science *28*, 1015-1048.

Kushwaha, A., Maurya, S., Pathak, R.K., Agarwal, S., Chaurasia, P.K., and Singh, M.P. (2018). Laccase From White Rot Fungi Having Significant Role in Food, Pharma, and Other Industries. In Research Advancements in Pharmaceutical, Nutritional, and Industrial Enzymology (Hersey: Igi Global), pp. 253-277.

Liu, Z.-g., Wang, H.-h., and Xue, C.-b. (2018). Molecular identification and enzymatic properties of laccase2 from the diamondback moth Plutella xylostella (Lepidoptera: Plutellidae). Journal of Integrative Agriculture *17*, 2310-2319.

Madzak, C., Mimmi, M.C., Caminade, E., Brault, A., Baumberger, S., Briozzo, P., Mougin, C., and Jolivalt, C. (2006). Shifting the optimal pH of activity for a laccase from the fungus *Trametes versicolor* by structure-based mutagenesis. Protein Engineering, Design and Selection *19*, 77-84.

Manzano-Nicolas, J., Marin-Iniesta, F., Taboada-Rodriguez, A., Garcia-Canovas, F., Tudela-Serrano, J., and Muñoz-Muñoz, J.L. (2020). Development of a method to measure laccase activity on methoxyphenolic food ingredients and isomers. International Journal of Biological Macromolecules *151*, 1099-1107.

Morris, G.M., Huey, R., Lindstrom, W., Sanner, M.F., Belew, R.K., Goodsell, D.S., and Olson, A.J. (2009). AutoDock4 and AutoDockTools4: Automated docking with selective receptor flexibility. Journal of Computational Chemistry *30*, 2785-2791.

Munoz, J.L., Garcia-Molina, F., Varon, R., Rodriguez-Lopez, J.N., Garcia-Canovas, F., and Tudela, J. (2006). Calculating molar absorptivities for quinones: Application to the measurement of tyrosinase activity. Analytical Biochemistry *351*, 128-138.

Piontek, K., Antorini, M., and Choinowski, T. (2002). Crystal structure of a laccase from the fungus *Trametes versicolor* at 1.90-angstrom resolution containing a full complement of coppers. Journal of Biological Chemistry *277*, 37663-37669.

Polyakov, K.M., Gavryushov, S., Fedorova, T.V., Glazunova, O.A., and Popov, A.N. (2019). The subatomic resolution study of laccase inhibition by chloride and fluoride anions using single-crystal serial crystallography: insights into the enzymatic reaction mechanism. Acta Crystallographica Section D-Structural Biology *75*, 804-816.

Raseda, N., Hong, S., Kwon, O.Y., and Ryu, K. (2014). Kinetic evidence for the interactive inhibition of laccase from *Trametes versicolor* by pH and chloride. Journal of Microbiology and Biotechnology *24*, 1673-1678.

Rodriguez-Lopez, J.N., Gilabert, M.A., Tudela, J., Thorneley, R.N.F., and Garcia-Canovas, F. (2000). Reactivity of horseradish peroxidase compound II toward substrates: Kinetic evidence for a two-step mechanism. Biochemistry *39*, 13201-13209.

Rulíšek, L., and Ryde, U. (2013). Theoretical studies of the active-site structure, spectroscopic and thermodynamic properties, and reaction mechanism of multicopper oxidases. Coordination Chemistry Reviews *257*, 445-458.

Sakurai, T., and Kataoka, K. (2007). Basic and applied features of multicopper oxidases, CueO, bilirubin oxidase, and laccase. The Chemical Record *7*, 220-229.

Sanner, M.F. (1999). Python: A programming language for software integration and development. Journal of Molecular Graphics & Modelling *17*, 57-61.

Serna Rodriguez, P., Rodriguez Lopez, J.N., Tudela, J., Varon, R., and Garcia Canovas, F. (1990). Effect of pH on the oxidation pathway of alpha-methyldopa catalysed by tyrosinase. The Biochemical journal *272*, 459-463.

Shleev, S., Andoralov, V., Falk, M., Reimann, C.T., Ruzgas, T., Srnec, M., Ryde, U., and Rulíšek, L. (2012). On the possibility of uphill intramolecular electron transfer in multicopper oxidases: electrochemical and quantum chemical study of bilirubin oxidase. Electroanalysis *24*, 1524-1540.

Shogo, T., Shogo, S., Tomihiro, N., and Fukiko, Y. (1993). Factors influencing the antioxidant activities of phenols by an Ab initio study. Bulletin of the Chemical Society of Japan *66*, 299-304.

Suderman, R.J., Dittmer, N.T., Kanost, M.R., and Kramer, K.J. (2006). Model reactions for insect cuticle sclerotization: Cross-linking of recombinant cuticular proteins upon their laccase-catalyzed oxidative conjugation with catechols. Insect Biochemistry and Molecular Biology *36*, 353-365.

Sugumaran, M., and Barek, H. (2016). Critical analysis of the melanogenic pathway in insects and higher animals. International Journal of Molecular Sciences *17*, 1753.

Wallace, A.C., Laskowski, R.A., and Thornton, J.M. (1995). LIGPLOT: a program to generate schematic diagrams of protein-ligand interactions. Protein Engineering, Design and Selection *8*, 127-134.

Yatsu, J., and Asano, T. (2009). Cuticle laccase of the silkworm, Bombyx mori: Purification, gene identification and presence of its inactive precursor in the cuticle. Insect Biochemistry and Molecular Biology *39*, 254-262.

Zhang, Y., Fan, J., Francis, F., and Chen, J. (2018). Molecular characterization and gene silencing of Laccase 1 in the grain aphid, Sitobion avenae. Archives of Insect Biochemistry and Physiology *97*.

Tables

Table 1. Kinetic constants of the oxidation of catecholamines and related compounds by laccase.

Substrate	K_M^S (mM)	V_{max}^S (μM/s)	V_{max}^S/K_M^S (1/h)	ΔG (kcal/mol)	K_d (mM)	δ_3 (ppm)	δ_4 (ppm)
DL-Isoprenaline[1]	0.39±0.04	0.59±0.02	5.44±0.40	-5.31	0.128	146.9	146.8
L-Isoprenaline[1]	0.54±0.05	0.56±0.02	3.75±0.36	-4.98	0.223	146.9	146.8
DL-α-MethylDopa	1.22±0.22	3.13±0.18	7.14±0.58	-4.39	0.603	146.7	146.0
L-α-MethylDopa	1.28±0.12	3.22±0.11	7.52±0.34	-4.43	0.564	146.7	146.2
L-Dopa methyl ester[1]	0.44±0.03	1.21±0.02	9.87±0.26	-4.27	0.739	146.9	146.2
L-Dopa	0.98±0.11	2.04±0.08	7.46±0.41	-3.96	1.247	146.9	146.2
Dopamine[1]	0.43±0.03	4.86±0.08	41.07±0.29	-4.86	0.273	146.8	145.6
L-Norpinephrine[1]	1.09±0.10	1.94±0.07	6.41±0.35	-4.64	0.396	144.0	144.0
L-Epinephrine[1]	0.68±0.04	1.82±0.03	9.66±0.22	-4.66	0.382	143.7	143.7

Michaelis-Menten constant of target substrate (K_M^S), maximum velocity of target substrate (V_{max}^S), power catalytic (V_{max}^S/K_M^S), binding energies (ΔG), equilibrium dissociation constant (K_d), chemical shift value to C-3 (δ_3) and C-4 (δ_4). [1]hydrochloride commercial reagent, K_M^S and V_{max}^S amended according to Eq. [8SM] and Eq. [9SM].

Figure Captions.

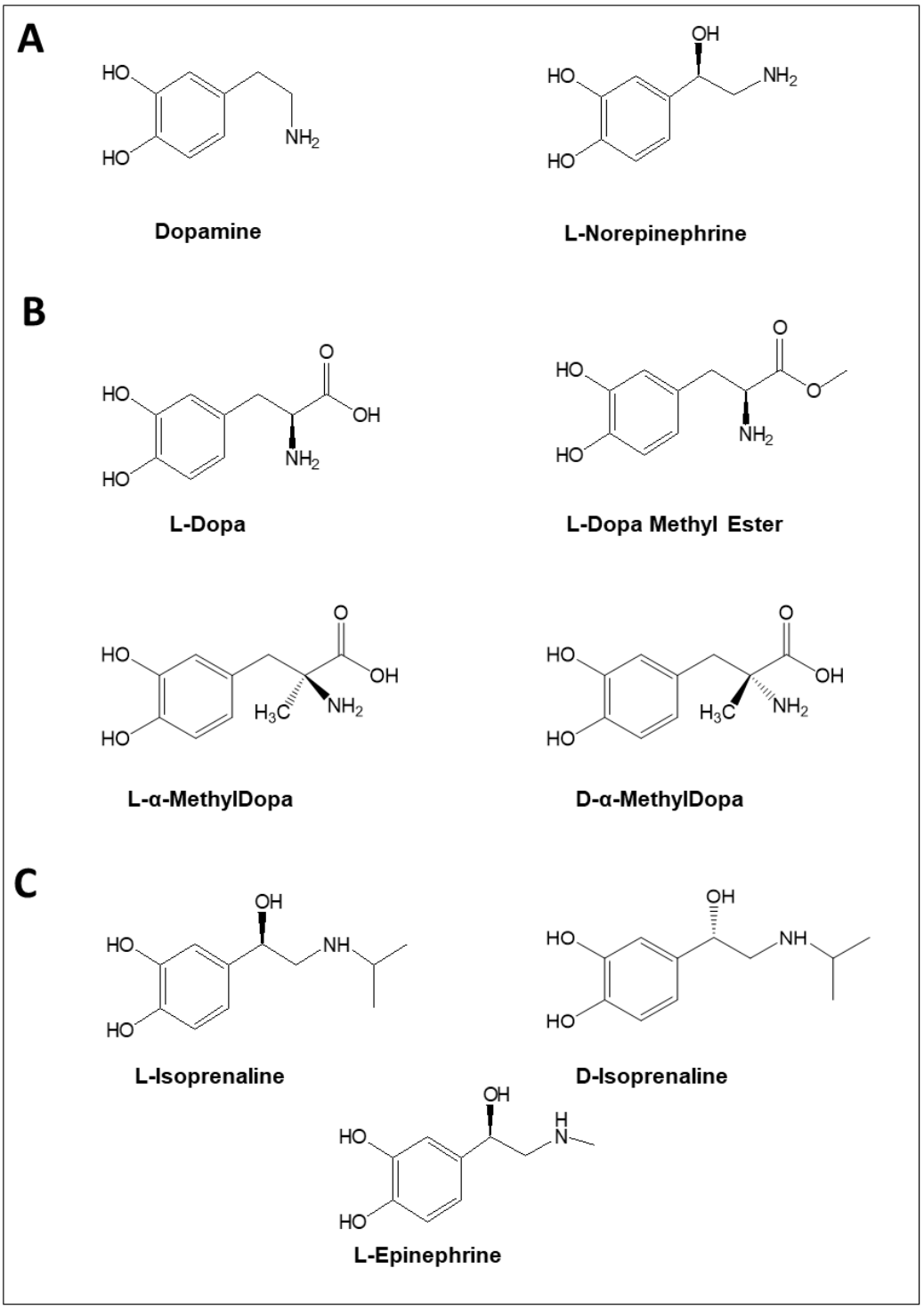

Fig. 1. Chemical structures of catecholamines and related compounds.

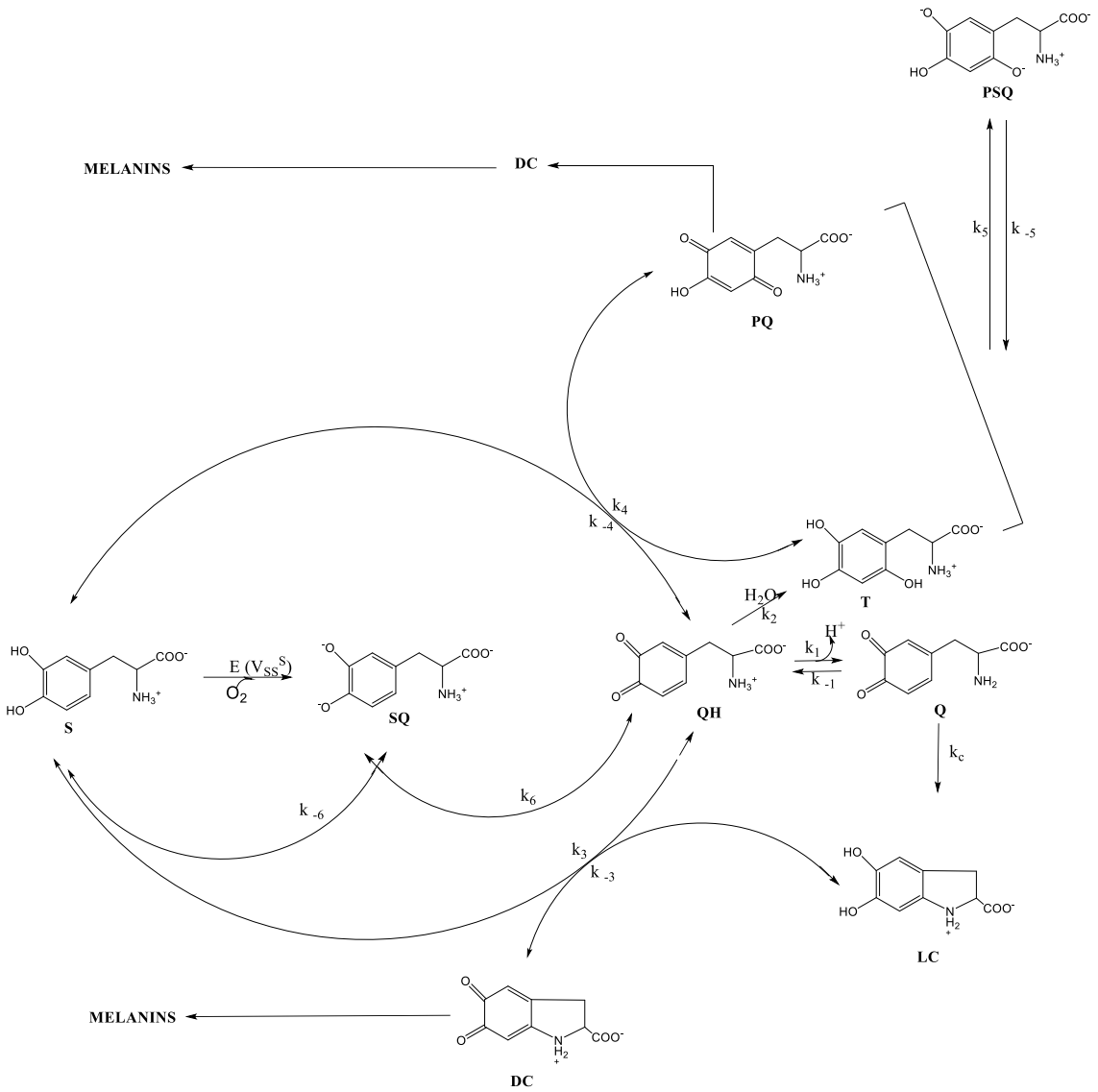

Fig. 2. Pathway proposed for the oxidation of L-dopa catalysed by laccase. Where: E is laccase; S = L-dopa; SQ = *o*-dopasemiquinone; QH = protonated *o*-dopaquinone; Q = deprotonated *o*-dopaquinone; LC = leucodopachrome; T = Topa; PQ = *p*-topaquinone; PSQ = *p*-topasemiquinone; DC = dopachrome.

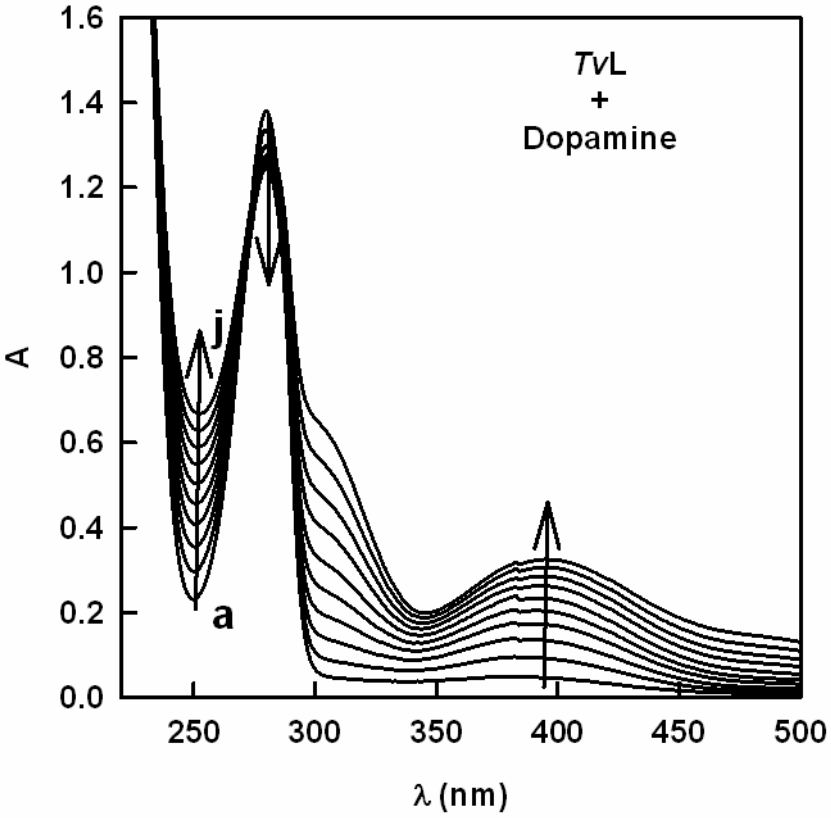

Fig.3

Fig. 3. Absorbance spectra of the action of laccase on dopamine. The experimental conditions were $[dopamine]_0$ = 0.57 mM and enzyme 15 μg/mL. Scans were made every minute (a-j). In λ=280 nm, maximum dopamine absorbance decreases. However, the absorbance for the reaction products increases in λ = 250 nm and 400 nm.

Fig. 4. Preliminary assays to qualitatively verify the presence of chemical pathway in the different substrates under study. Catecholamines and related substrates were assayed with *Trametes versicolor* laccase, being measured the increase in absorbance at 475 nm. Reaction conditions at 25ºC were 50 mM acetate buffer pH 4.

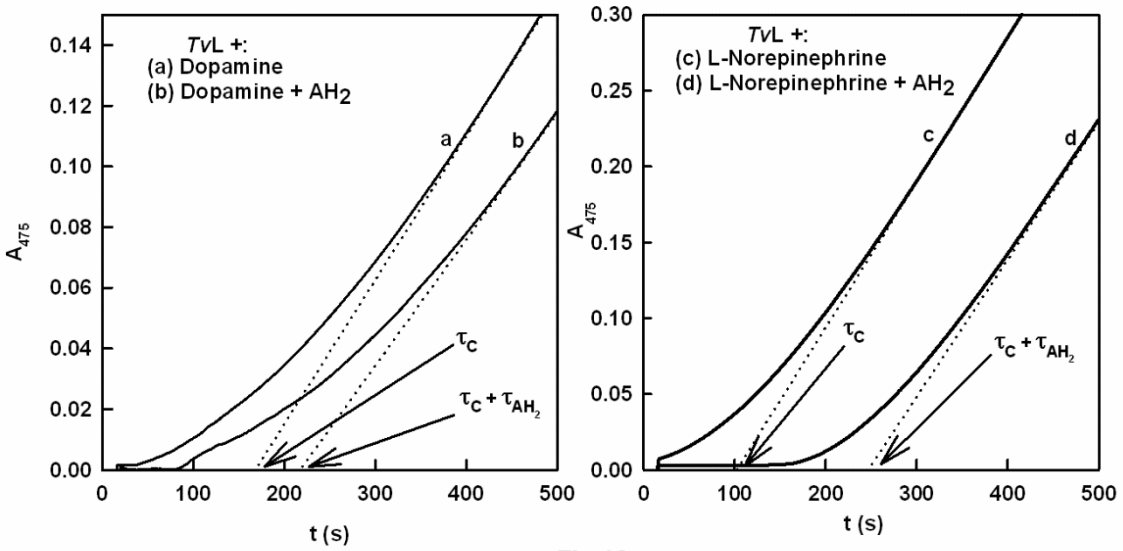

Fig.4A

A. Chronometric method for measuring laccase activity. Absorbance recordings at 475 nm of product formation over time. Experimental conditions were: Left side. (a) $[\text{Dopamine}]_0$ = 2.83 mM and 17 µg/mL *Tv*L; (b) Same than (a) with $[AH_2]_0$= 70 µM. Right side. L-Norepinephrine, (c) $[\text{L-Norepinephrine}]_0$ = 1.5 mM and 17 µg/mL *Tv*L; (d) Same than (c) with $[AH_2]_0$= 80 µM.

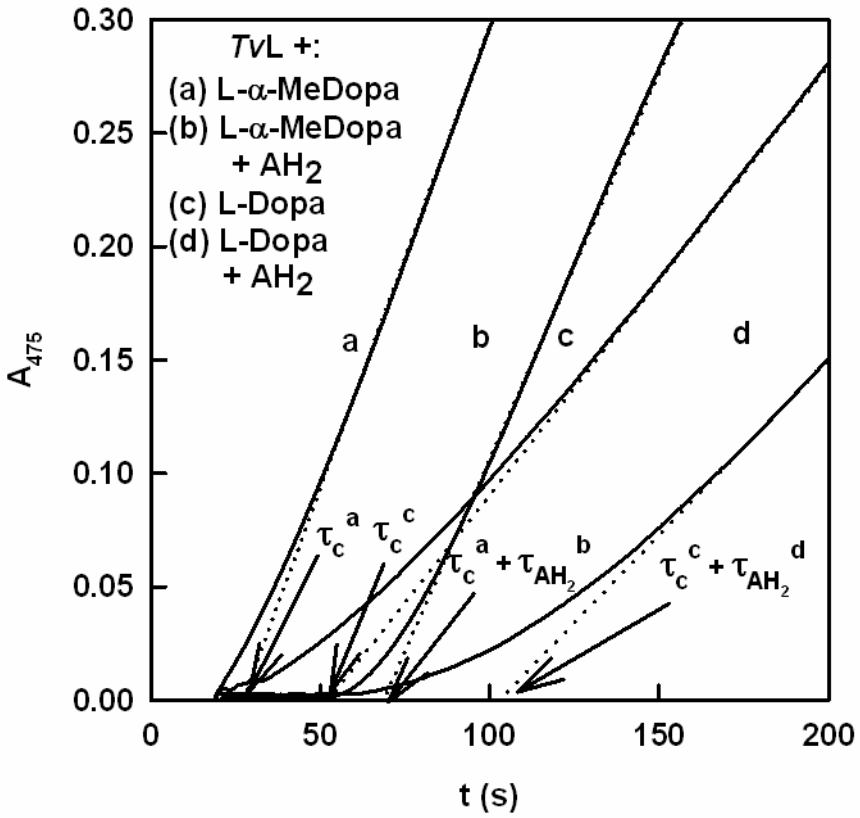

Fig.4B

B. Chronometric method for measuring laccase activity. Absorbance recording at 475 nm of product formation overtime. Experimental conditions were: (a) $[L\text{-}\alpha\text{-}MeDopa]_0$ = 6.7 mM and 17 µg/mL *Tv*L; (b) Same than (a) with $[AH_2]_0$=60 µM. (c) L-dopa oxidation by laccase in absence of AH_2. Experimental conditions were: $[L\text{-}Dopa]_0$ = 3.8 mM and 8.5 µg/mL *Tv*L; (d) Same than (c) with $[AH_2]_0$= 20 µM.

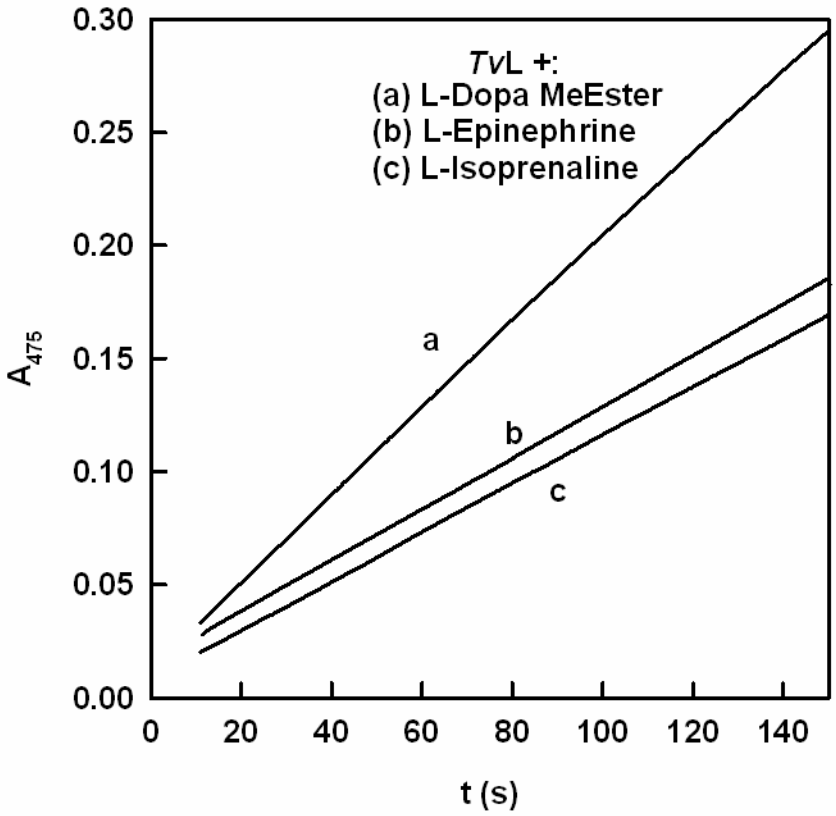

Fig.4C

C. Chronometric method for measuring laccase activity. Absorbance recordings at 475 nm of product formation over time. Experimental conditions were: *Tv*L Laccase 17 µg/mL, (a) 2 mM L-epinephrine, (b) 1.8 mM L-dopa methyl ester, (c) 1.6 mM L-isoprenaline.

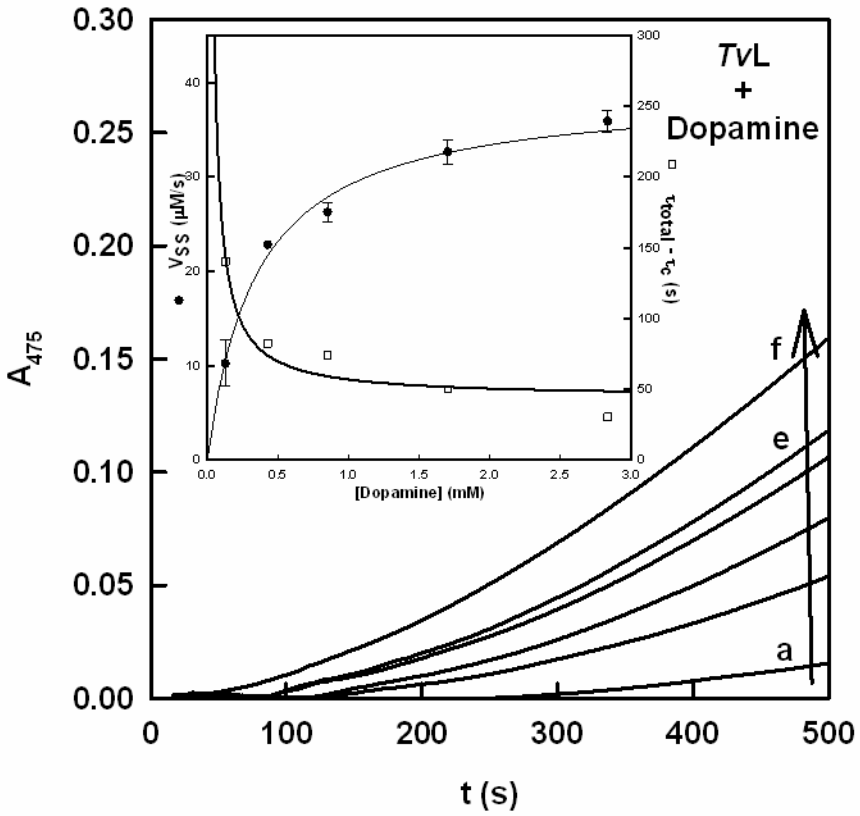

Fig.5

Fig. 5. Chronometric method for measuring laccase activity on dopamine. Absorbance recordings at 475 nm of product formation over time. Experimental conditions were: Acetate buffer 50 mM pH 4, $[AH_2]_0$ = 70 μM, $[E]_0$ = 17 μg/mL, and $[Dopamine]_0$ = 0.13-2.83 mM (a-e). (f) Equal conditions than (e) without ascorbic acid. Insert: representation of $\tau_{total} - \tau_c = \tau_{AH_2}$ (□) and V_{SS}(●) with respect to dopamine concentration.

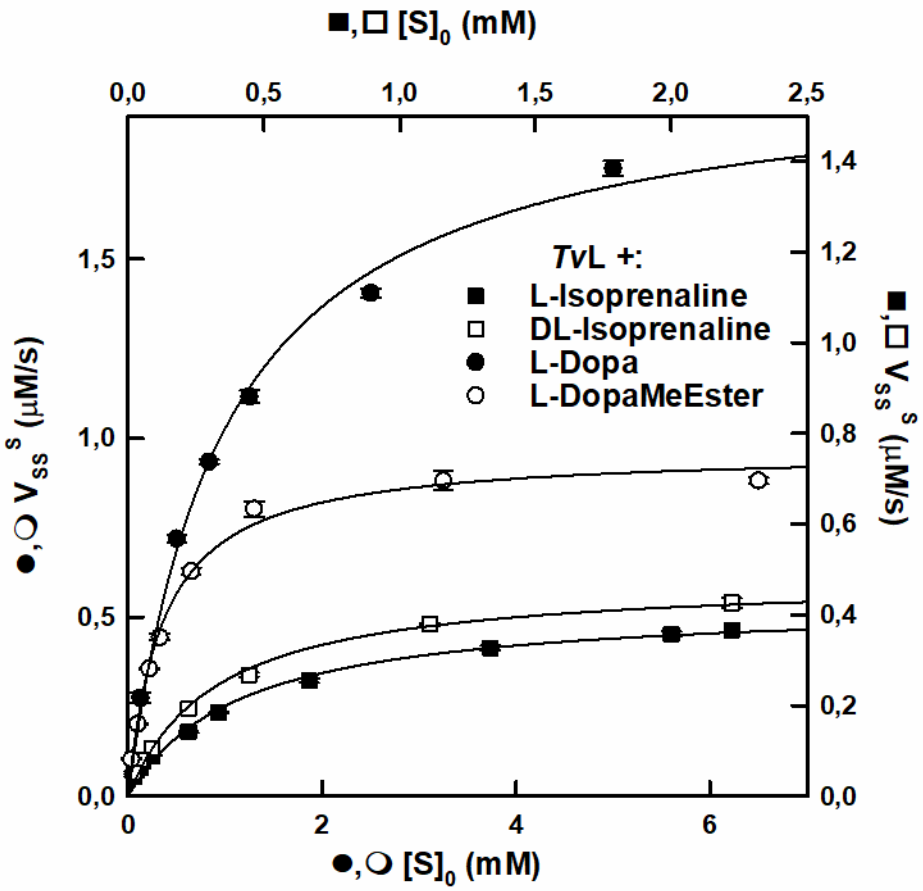

Fig.6

Fig. 6. Kinetic characterization of different substrates. Representation of initial steady-state rates (V_{SS}^{S}) obtained by the chronometric method in laccase (T*vL* 17 µg/mL) action on (■) **L-Isoprenaline**; $[AH_2]_0$ = 30 µM. (□) **DL-Isoprenaline**; $[AH_2]_0$ = 30 µM. (●) **L-Dopa**; $[AH_2]_0$ = 50 µM. (○) **L-DopaMeEster**, $[AH_2]_0$ = 50 µM.

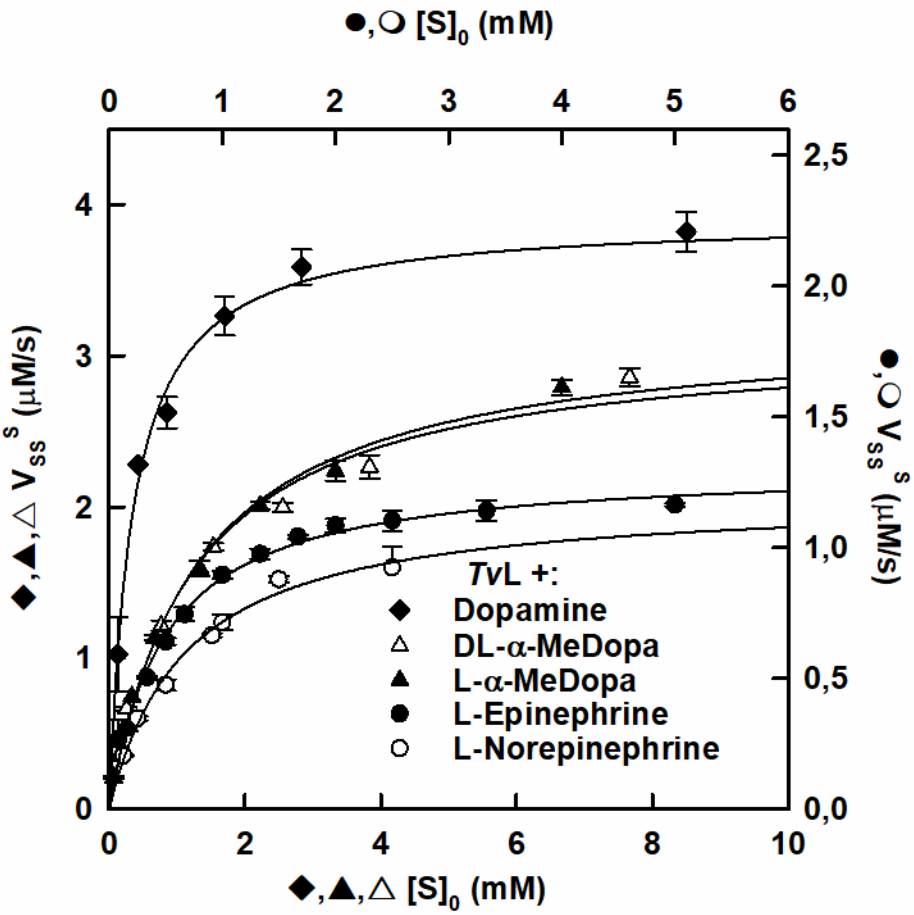

Fig.7

Fig. 7. Kinetic characterization of different substrates. Representation of initial steady-state rates (V_{SS}^{S}) obtained by the chronometric methods in laccase (T*vL* 17 μg/mL) action on (◆) **Dopamine**; $[AH_2]_0$ = 70 μM. (△) **DL-α-MeDopa**; $[AH_2]_0$ = 40 μM. (▲) **L-α-MeDopa**; $[AH_2]_0$ = 85 μM. (●) **L-Epinehrine**; $[AH_2]_0$ = 80 μM. (○) **L-Norepinehrine**; $[AH_2]_0$ = 80 μM.

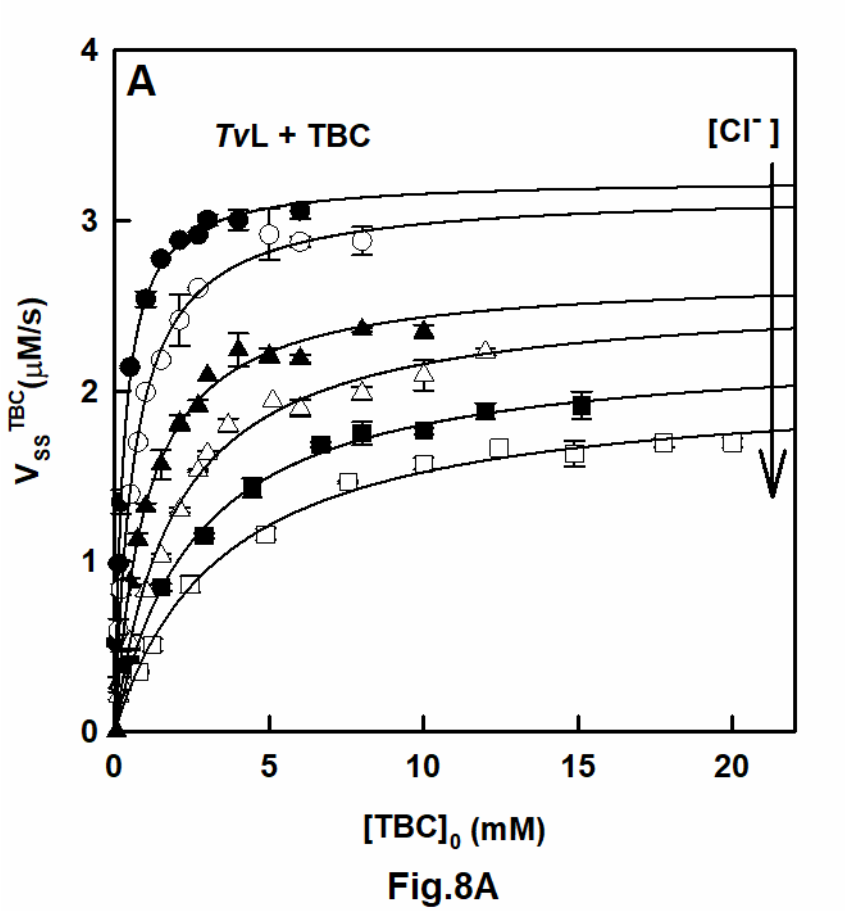

Fig. 8. **A**. *Tv*L inhibition by chloride. Representation of steady-state rate vs substrate concentration $[TBC]_0$ in the action of laccase (T*vL* 17 μg/mL) on TBC (V_{SS}^{TBC}) . Experimental conditions were (●) $[TBC]_0$ =0.06-6 mM, $[Cl^-]_0$= 0 Mm; (○) $[TBC]_0$ =0.12-8, $[Cl^-]_0$= 2.5 mM; (▲) $[TBC]_0$ =0.12-10, $[Cl^-]_0$= 5 mM; (△) $[TBC]_0$ =0.12-12, $[Cl^-]_0$= 10 mM; (■) $[TBC]_0$ =0.51-15, $[Cl^-]_0$= 20 mM; (□) $[TBC]_0$ =0.8-20, $[Cl^-]_0$= 30 mM.

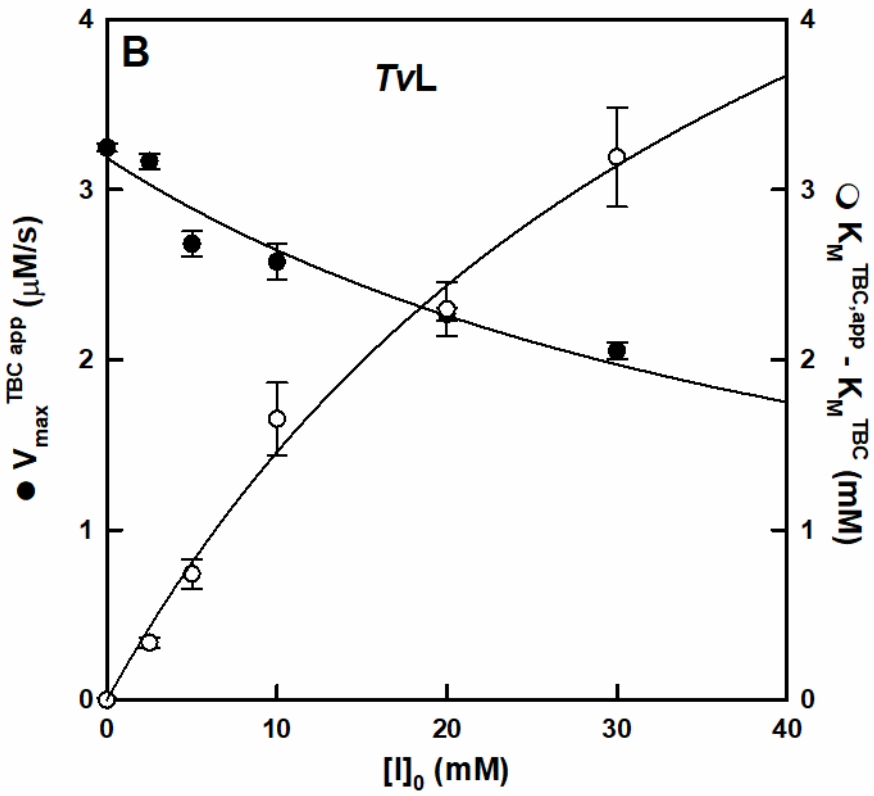

Fig.8B

Fig. 8B. Calculation of K_I and K_I'. Representation of the values of $V_{max}^{TBC\ app}$ (●) and $K_M^{TBC\ app} - K_M^{TBC}$ (○) obtained at different concentrations of inhibitor (Cl^-) and fit by nonlinear regression of $V_{max}^{TBC\ app}$ to Eq.[2SM] and $K_M^{TBC\ app} - K_M^{TBC}$ to Eq.[4SM].

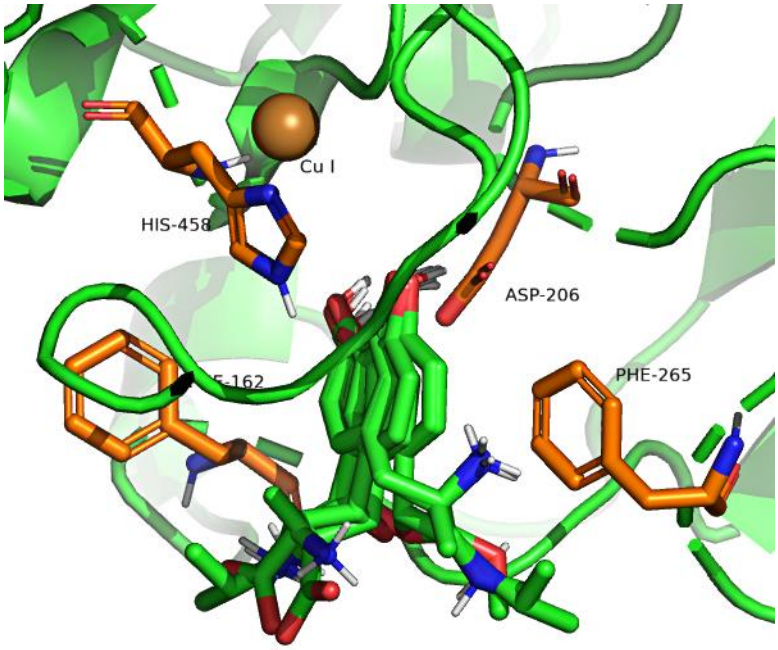

Fig. 9. Docked conformations of all ligands studied, over the laccase **1GYC** model. The conformers only include polar hydrogens. The brown sphere corresponds to T1 copper. Carbon backbone is depicted in green in the ligands and in orange in the laccase residues.

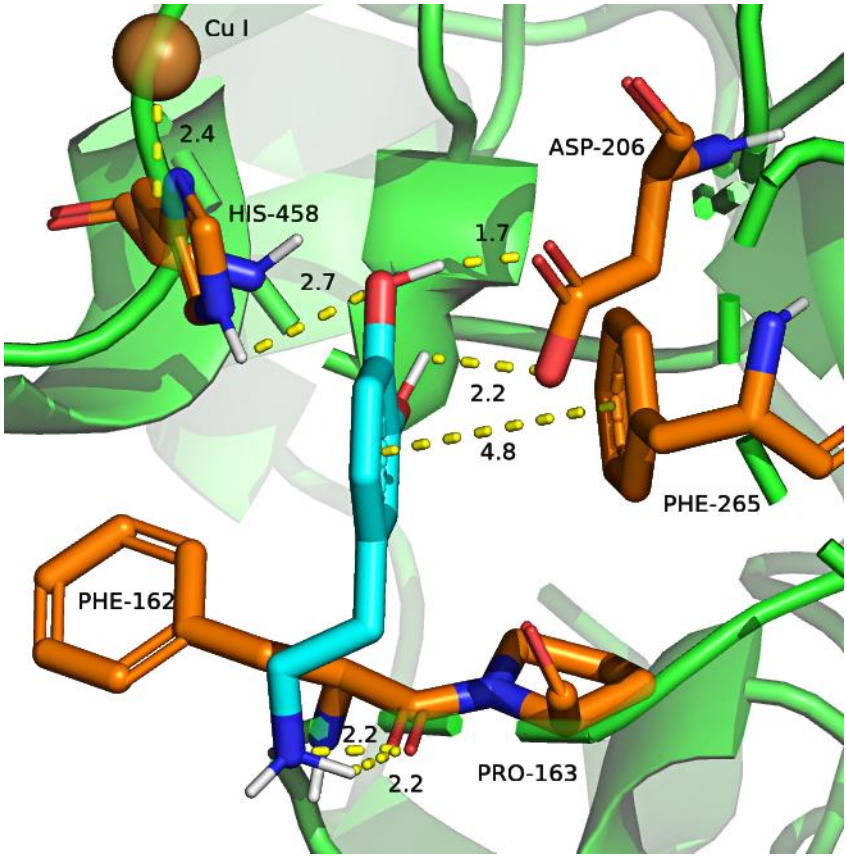

Fig. 10. Docked conformations of dopamine. Only polar hydrogens are shown in the structures. The brown sphere corresponds to T1 copper. Carbon backbone is depicted in blue in dopamine and in orange in the laccase residues (**1GYC**).

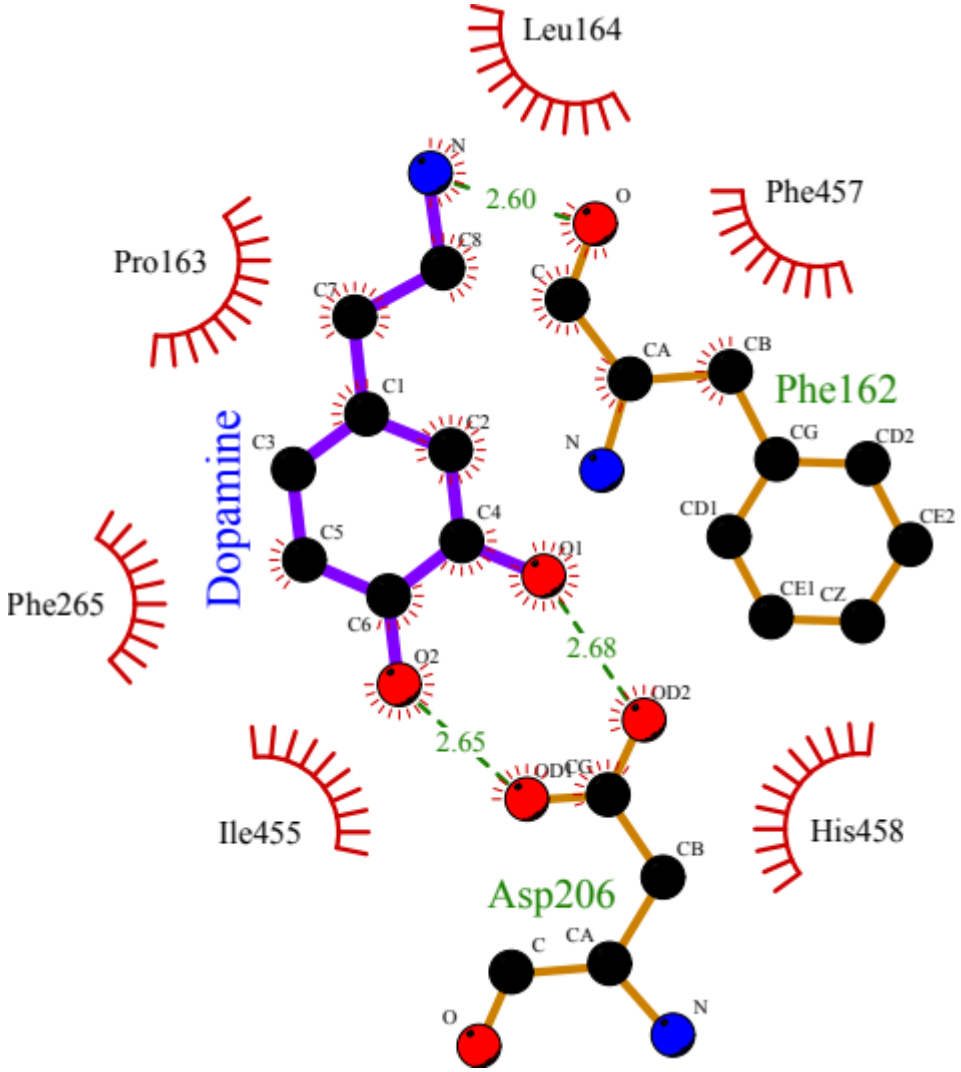

Fig. 11. Two-dimensional docked conformation of dopamine. The atoms of oxygen, carbon, and nitrogen are colored by red, black, and blue respectively. The purple solid lines stand for dopamine, while orange solid lines stand for amino acid residues belonged to laccase (**1GYC**). The dotted lines show the hydrogen bonds including the bond length (Å). The models in red solid wires are denoted as hydrophobic contacts in the binding of laccase to dopamine.

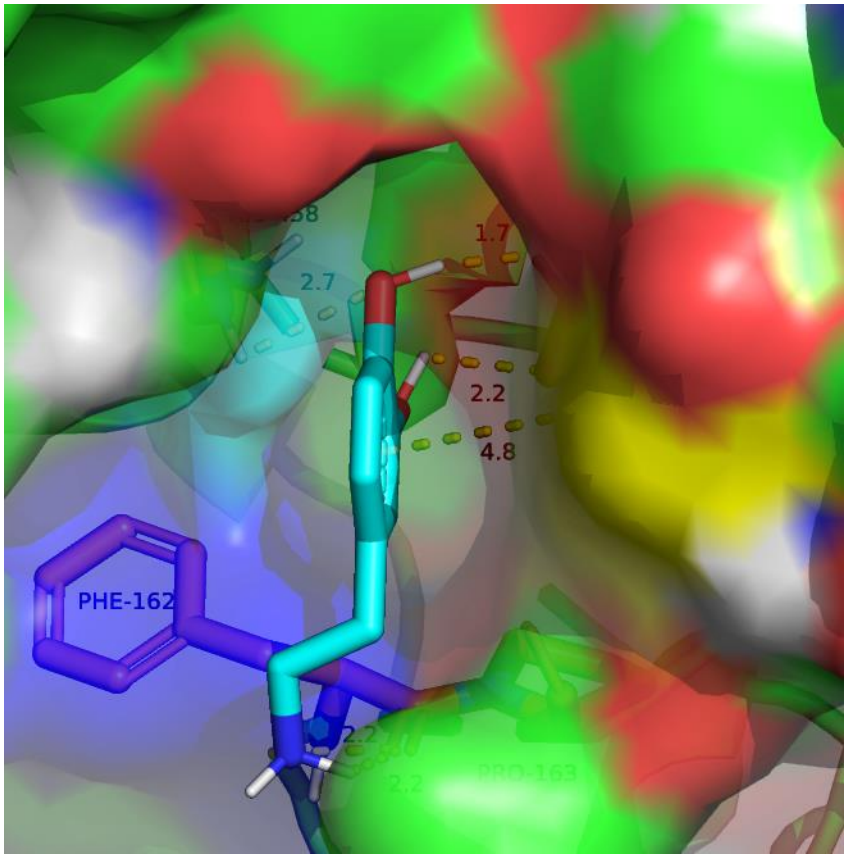

Fig. 12. Docking structure on the molecular surface model corresponding to **Fig. 10**.

Supplementary Material

Laccase inhibition by chloride.

The proposed mechanism to explain the inhibition of laccase by chloride is the one shown in Fig. 1SM.

Applying the steady-state approximation to the action of laccase on TBC, the expression of the velocity is obtained (V_{SS}^{TBC}).

$$V_{SS}^{TBC} = \frac{\frac{V_{max}^{TBC}}{1+\frac{[I]_0}{K_I'}}[TBC]_0}{K_M\frac{1+\frac{[I]_0}{K_I}}{1+\frac{[I]_0}{K_I'}}+[TBC]_0} \qquad (1SM)$$

Experimental design for the characterization of the inhibitor: Determination of K_I and K_I'.

Step 1. Laccase kinetics with 4-tert-butylcatechol. Determination of K_M^{TBC} and V_{max}^{TBC}.

Step 2. Kinetic at different concentrations of inhibitor. Determination of $K_M^{TBC\,app}$ and $V_{max}^{TBC\,app}$.

Step 3. $V_{max}^{TBC\,app}$ analysis regarding the inhibitor concentration by non-linear regression, according to the equation (2SM). Determination of K_I'.

$$V_{max}^{TBC\,app} = \frac{K_I'\ V_{max}^{TBC}}{K_I'+[I]_0} \qquad (2SM)$$

Step 4. $K_M^{TBC\ app}$ dependence regarding the inhibitor concentration is:

$$K_M^{TBC\ app} = \frac{K_M^{TBC} K_I' + \frac{K_M^{TBC} K_I'}{K_I}[I]_0}{K_I' + [I]_0} \quad (3SM)$$

Regrouping the Eq. [3SM], we obtain:

$$K_M^{TBC\ app} - K_M^{TBC} = \frac{K_M^{TBC}\left(\frac{K_I'}{K_I} - 1\right)[I]_0}{K_I' + [I]_0} \quad (4SM)$$

Nonlinear regression analysis of $K_M^{TBC\ app} - K_M^{TBC}$ *vs.* $[I]_0$, allows obtaining K_I.

Mixed-inhibition of laccase by chloride when the substrate is stoichiometric with the inhibitor.

Most of the substrates shown in Fig. 1 and Table1 are in the hydrochloride form, therefore when the substrate is varied; it is simultaneously varied in the same concentration of inhibitor. So that, $[S]_0 = [I]_0$. From Eq. [1SM], if $[I]_0$ is substituted by $[S]_0$, we obtain:

$$V_{SS}^S = \frac{V_{max}^S [S]_0}{K_M^S + \left(1 + \frac{K_M^S}{K_I}\right)[S]_0 + \frac{[S]_0^2}{K_I'}} \quad (5SM)$$

$$V_{SS}^S = \frac{V_{max}^S K_I' [S]_0}{K_M^S K_I' + K_I'\left(1 + \frac{K_M^S}{K_I}\right)[S]_0 + [S]_0^2} \quad (6SM)$$

Working at low concentrations of substrate, the quadratic term in the denominator can be depreciated and from Eq. [6SM] we get:

$$V_{SS}^{S} = \frac{\frac{V_{max}^{S}}{1+\frac{K_M^S}{K_I}}[S]_0}{\frac{K_M^S}{1+\frac{K_M^S}{K_I}}+[S]_0} = \frac{V_{max}^{S,app}[S]_0}{K_M^{S,app}+[S]_0} \quad (7SM)$$

Step 5. Non-linear regression of V_{SS}^{S} *vs.* $[S]_0$ allows to obtain, according to Eq.[7SM]:

$$K_M^{S,app} = \frac{K_M^S}{1+\frac{K_M^S}{K_I}} \quad (8SM)$$

And

$$V_{max}^{S,app} = \frac{V_{max}^{S}}{1+\frac{K_M}{K_I}} \quad (9SM)$$

From Eq. [8SM], taking into consideration the K_I values, K_M^S for each substrate can be obtained (see Table 1)

From Eq. [9SM], taking into consideration the values for K_M^S and K_I, the value of V_{max}^{S} for each substrate can be obtained. This methodology allowed characterizing all the laccase as shown in Table 1.

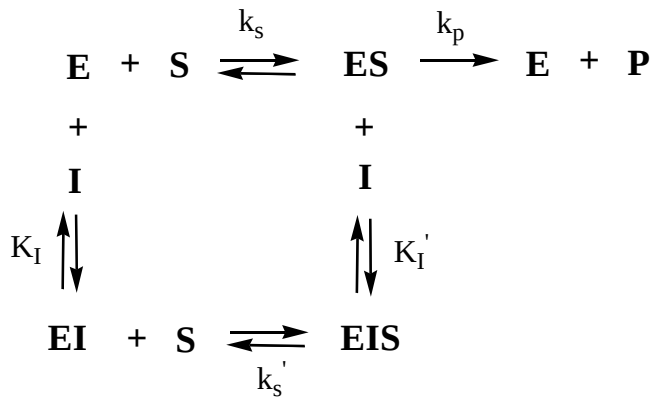

Fig. 1SM. Mechanism proposed for the mixed inhibition of laccase by chloride, where: E is laccase, S, is an enzyme substrate, I is chloride and P is the reaction product.

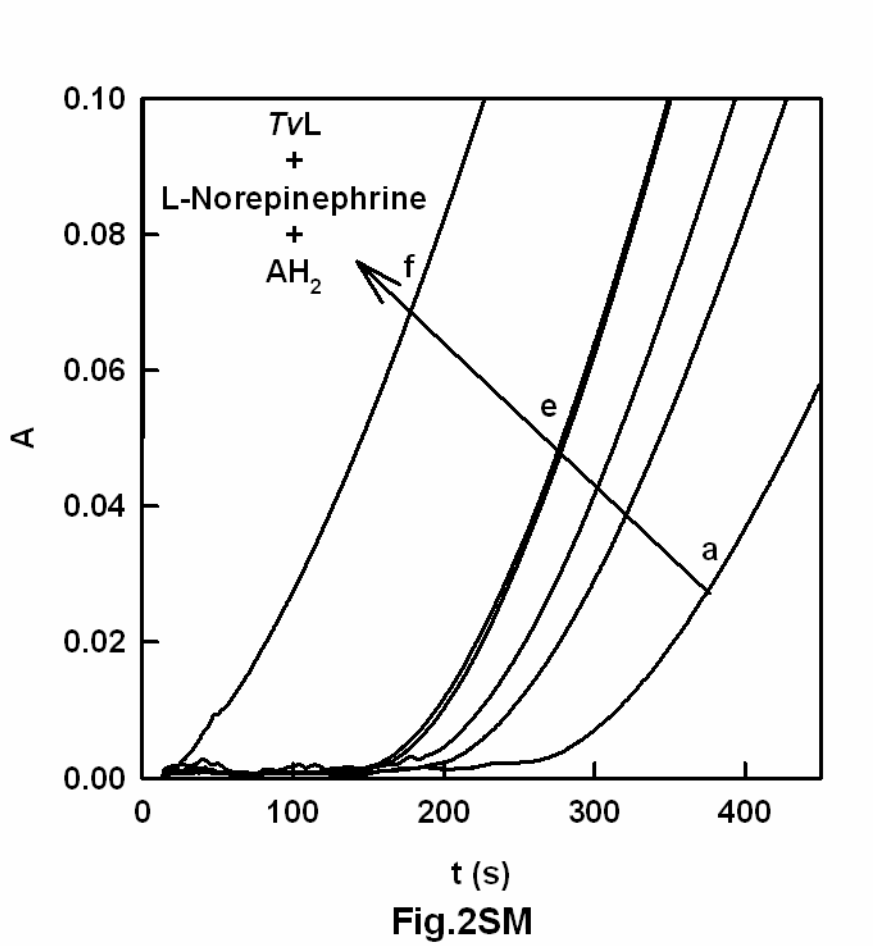

Fig. 2SM. Chronometric method for measuring laccase activity on L-Norepinephrine. Absorbance recordings at 475 nm of product formation over time. Experimental conditions were: $[AH_2]_0$ = 80 µM, $[E]_0$ = 17 µg/mL, and $[\text{L-Norepinephrine}]_0$ = 0.5-2 mM (a-e). (f) Equal conditions than (d = 1.5 mM) without ascorbic acid.

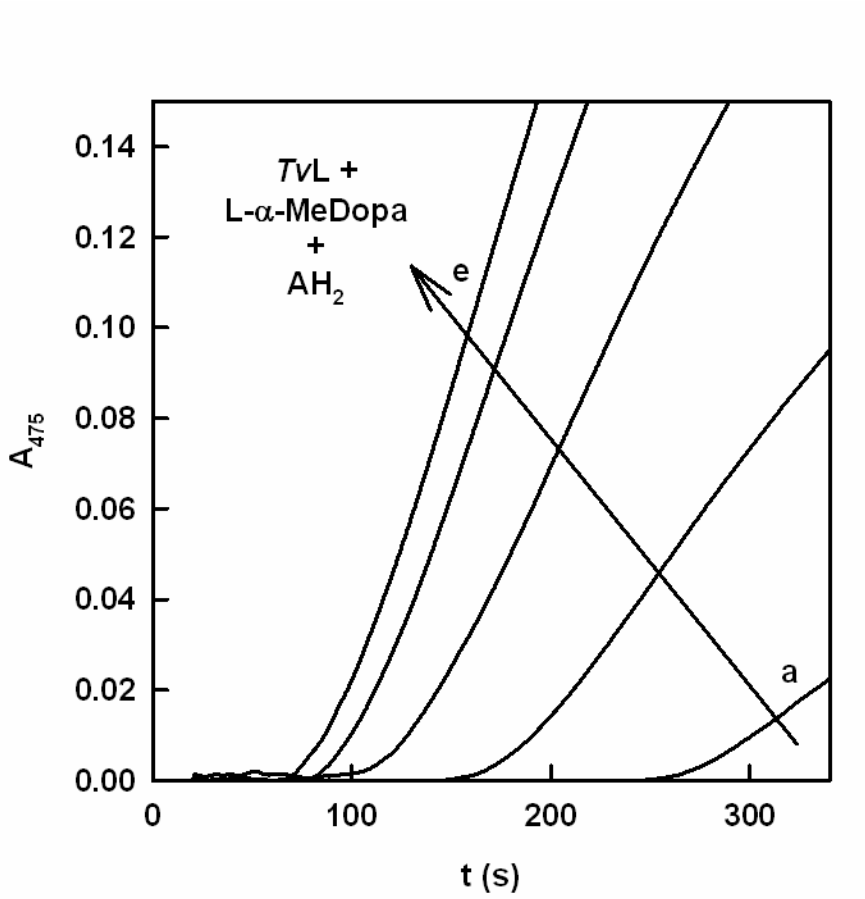

Fig.3SM

Fig. 3SM. Chronometric method for measuring laccase activity on L-α-MeDopa. Absorbance recordings at 475 nm of product formation over time. Experimental conditions were: $[AH_2]_0$ = 40 µM, $[E]_0$ = 17 µg/mL, and $[L\text{-}\alpha\text{-MeDopa}]_0$ = 0.33-3.33 mM (a-e).

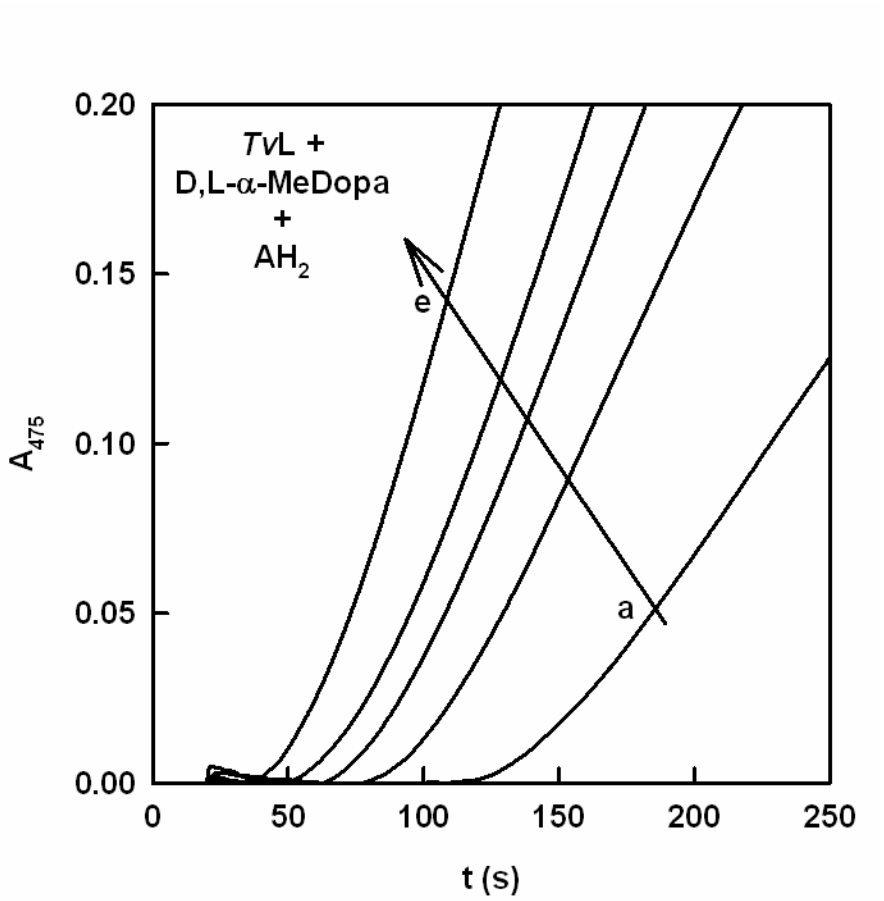

Fig.4SM

Fig. 4SM. Chronometric method for measuring laccase activity on DL-α-MeDopa. Absorbance recordings at 475 nm of product formation over time. Experimental conditions were: 50 mM Acetate buffer pH 4, $[AH_2]_0$ = 40 µM, $[E]_0$ = 17 µg/mL, and $[DL\text{-}\alpha\text{-}MeDopa]_0$ = 0.77-7.67 mM (a-e).

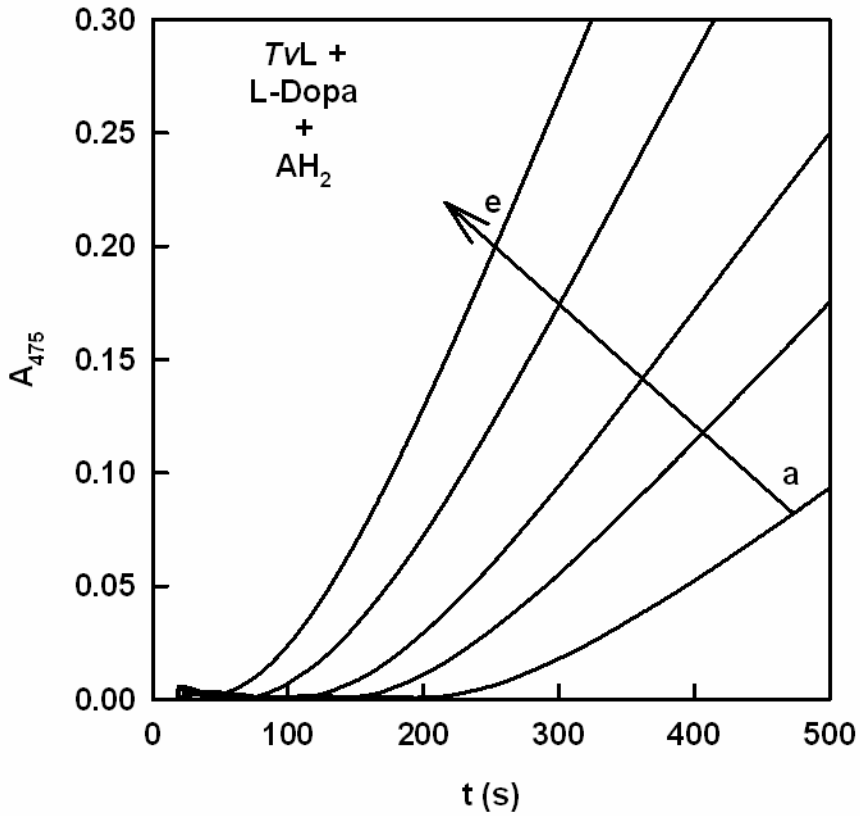

Fig.5SM

Fig. 5SM. Chronometric method for measuring laccase activity on L-Dopa. Absorbance recordings at 475 nm of product formation over time. Experimental conditions were: $[AH_2]_0$ = 40 µM, $[E]_0$ = 17 µg/mL, and $[L\text{-Dopa}]_0$ = 0.5-5 mM (a-e).

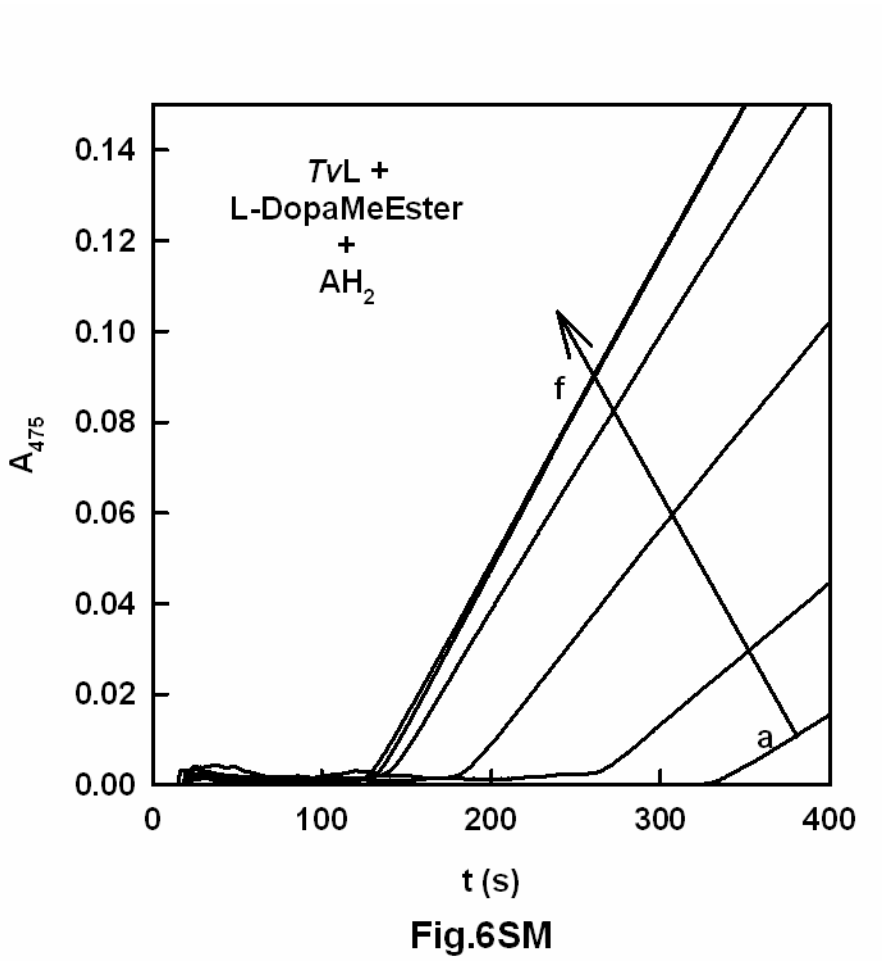

Fig. 6SM. Chronometric method for measuring laccase activity on L-DopaMeEster. Absorbance recordings at 475 nm of product formation over time. Experimental conditions were: $[AH_2]_0$ = 50 µM, $[E]_0$ = 17 µg/mL, and $[\text{L-DopaMeEster}]_0$ = 0.22-6.5 mM (a-e).

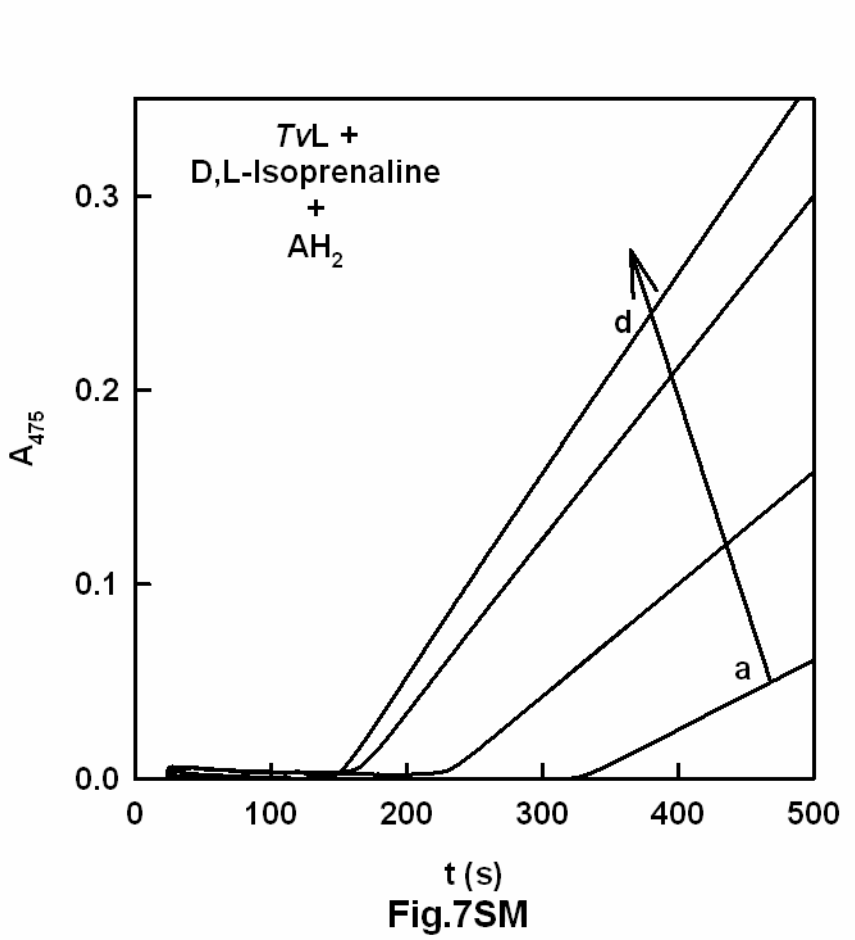

Fig.7SM. Chronometric method for measuring laccase activity on DL-Isoprenaline. Absorbance recordings at 475 nm of product formation over time. Experimental conditions were: $[AH_2]_0$ = 30 µM, $[E]_0$ = 17 µg/mL, and [DL-Isoprenaline]$_0$ = 0.02-2.2 mM (a-d).

Author contributions

J.M-N. and J.M-M. designed and directed the project and experiments. J.M-N. and A.T-D designed and performed the kinetic biochemical experiments. J.T-P performed the docking and structural biology experiments. F.G.-M. drafted all figures included in the manuscript and supplementary material. F.G.-C., F.M.-I., J.T-S. and J.M-M., analysed and interpreted the data. F.M.-I., F.G-C and J.M.-M., drafted the manuscript and figures, provided commentary and edits to the manuscript and figures and prepared the final version of the article.